Journal of Economic Dynamics & Control 117 (2020) 103926

Contents lists available at ScienceDirect

Journal of Economic Dynamics & Control

journal homepage: www.elsevier.com/locate/jedc

When the U.S. catches a cold, Canada sneezes: A lower-bound tale told by deep learning☆

Vadym Lepetyuk[a], Lilia Maliar[b], Serguei Maliar[c]

[a] Bank of Canada, 234 Wellington St., Ottawa, Ontario K1A 0G9, Canada
[b] The Graduate Center, CUNY, NY 10016, USA and CEPR
[c] Santa Clara University, 500 El Camino Real, Santa Clara, CA 95053, USA

ARTICLE INFO

Article history:
Received 20 September 2019
Revised 22 April 2020
Accepted 23 April 2020
Available online 21 May 2020

JEL classification:
C61
C63
C68
E31
E52

Keywords:
Central banking
Policymakers
ToTEM
bToTEM
Stochastic simulation
Machine learning
Deep learning
Supervised learning
Unsupervised learning
Neural networks
Ergodic set
Clustering analysis
Adaptive grid
Central bank
Bank of Canada
US Fed
Large-scale model
New Keynesian model
ZLB
ELB

ABSTRACT

The Canadian economy was not initially hit by the 2007-2009 Great Recession but ended up having a prolonged episode of the effective lower bound (ELB) on nominal interest rates. To investigate the Canadian the ELB experience, we build a "baby" ToTEM model – a scaled-down version of the Terms of Trade Economic Model (ToTEM) of the Bank of Canada. Our model includes 49 nonlinear equations and 21 state variables. To solve such a high-dimensional model, we develop a projection deep learning algorithm – a combination of unsupervised and supervised (deep) machine learning techniques. Our findings are as follows: The Canadian ELB episode was contaminated from abroad via large foreign demand shocks. Prolonged ELB episodes are easy to generate with foreign shocks, unlike with domestic shocks. Nonlinearities associated with the ELB constraint have virtually no impact on the Canadian economy but other nonlinearities do in particular, the degree of uncertainty and specific closing condition used to induce the model's stationarity.

☆ This paper is a revised version of Bank of Canada Staff Working Paper 2017-21. Lilia Maliar and Serguei Maliar acknowledge the support from NSF grants SES-1949413 and SES-1949430, respectively. The authors received useful comments and suggestions from researchers of the Bank of Canada, in particular, José Dorich, Stefano Gnocchi and Oleksiy Kryvtsov. HanJing Xie provided excellent research assistance. The authors are especially grateful to JEDC editor and two anonymous referees for many thoughtful and constructive critiques and suggestions. The views expressed in this paper are solely those of the authors and may differ from official Bank of Canada views. No responsibility for them should be attributed to the Bank of Canada.

E-mail addresses: lepetyuk@gmail.com (V. Lepetyuk), lmaliar@gc.cuny.edu (L. Maliar), smaliar@scu.edu (S. Maliar).

https://doi.org/10.1016/j.jedc.2020.103926
0165-1889/

1. Introduction

The Canadian economy did not experience a 2007 subprime crisis and was not initially hit by the Great Recession, unlike the U.S. and Europe; see a speech of the Bank of Canada Deputy Governor Boivin (2011). Nonetheless, after few months into the recession, Canada entered a prolonged episode of the effective lower bound (ELB) on nominal interest rates.[1] In the paper, we investigate a hypothesis that the ELB crisis was contaminated to Canada from abroad, in particular, from the U.S.

Bank of Canada has a well-developed macroeconomic model of the Canadian economy called the Terms of Trade Economic Model (ToTEM); see a technical report of Dorich et al. (2013). That model is huge – 356 equations and unknowns and 215 state variables – and is analyzed exclusively by linearization-based methods. In the paper, we construct a scaled-down version of ToTEM, which we call a "baby" ToTEM. The model is still very large: it includes 49 equations and 21 state variables. To solve it, we introduce a deep learning (DL) projection algorithm – a combination of unsupervised and supervised machine learning techniques – capable of constructing global, fully nonlinear solutions.

We calibrate the bToTEM model by following the ToTEM analysis as closely as possible, and we check that our scaled-down model reproduces remarkably well the impulse response functions of the full-scale model. We conduct two empirically relevant policy experiments related to the ELB episode in Canada during the Great Recession. In the first experiment, we introduce into bToTEM a sequence of foreign shocks from ToTEM; and in the second experiment, we analyze a change in the inflation target from 2 to 3 percent.

Our analysis delivers several interesting results. First, we demonstrate that the international transmission of ELB is empirically plausible mechanism for explaining the Canadian ELB experience. To be specific, in the beginning of the Great Recession, Canada faced a dramatic reduction in foreign demand (in particular, in the U.S. demand), and it proved sufficient to produce a prolonged ELB episode in a realistic and meticulously calibrated bToTEM model of the Canadian economy.

Second, we demonstrate that it is relatively easy to generate realistic ELB (or ZLB) episodes in new Keynesian models via the foreign shocks calibrated from the data. In contrast, it is difficult to produce realistic ELB episodes via domestic shocks which lead to comovements that are inconsistent with basic business-cycle facts. Thus, generating an appealing domestic ELB scenario is a challenge for bToTEM, like it is for other new Keynesian models studied in the literature.

Third, we find that the Canadian economy would entirely avoid the ELB episode if the target inflation rate were 3 instead of 2 percent. However, this finding must be taken with caution. Our analysis abstracts from the issue of credibility of inflation targeting, so achieving a higher inflation target in the model is straightforward. However, it seems questionable that central banks could easily meet an increased inflation target, given persistently low inflation in many developed economies in recent years despite high degrees of monetary accommodation.

Fourth and contrary to what we expected, we find that the ELB constraint plays a relatively minor role in the bToTEM's performance. In our baseline simulation, both local and global solution methods predict similar timing and duration of the ELB episodes. Furthermore, the presence of active ELB does not visibly affect the model's variables other than the interest rate. We argue that a modest role of ELB is due to the presence of rule-of-thumb firms and wage-unions in bToTEM. Such agents dampen excessive responses of the economy to future shocks, ameliorating the forward guidance puzzle. The nature of the ELB irrelevance result in our model is different from the one advocated in Debartoli et al. (2019). In their case, the ELB constraint does not affect the economy because of the availability of unconventional monetary policies (forward guidance, quantitative easing, etc.) while in our case, such constraint is not quantitatively significant due to the presence of the rule-of-thumb agents.

Fifth, we discover that other nonlinearities – those not associated with ELB – can play an important role in the model's predictions. In particular, when assessing the impact of a hypothetical transition from a 2 to 3 percent inflation target on the Canadian economy, we spot economically significant differences between the linear and nonlinear dynamics. We show that such differences are attributed to an uncertainty effect which implies large differences in steady states between linear and nonlinear solutions. The effect of uncertainty on the steady state is known in the literature but we show a simple way to control for such effect: if the initial condition for each solution is constructed in relation to its own steady state (which we view as a coherent approach), then the linear and nonlinear impulse responses look like vertical shifts of one another.

Finally and most strikingly, we find that the closing condition, used to ensure stationarity in open-economy models, plays an important role in the bToTEM dynamics. This finding is surprising because it is at odds with the well-known conclusion of Schmitt-Grohé and Uribe (2003) that closing conditions play virtually no role in the implications of the open-economy models. Our conclusion is different because the analysis of Schmitt-Grohé and Uribe (2003) relies on linearization while we focuses on nonlinear effects. In particular, in one experiment, we show that the closing conditions in linear and exponential forms lead to significantly different transitional dynamics. However, the linearized versions of these two closing conditions are identical, so the linearization analysis of Schmitt-Grohé and Uribe (2003) cannot differentiate between them. In turn, our nonlinear analysis reveals the importance of high-order terms, neglected by the linearization method.

The introduction of deep learning was critical for telling the nonlinear tale of the Canadian ELB episode.[2] Models like bToTEM are intractable under conventional value function iteration and projection methods due to the curse of

[1] ELB is similar to ZLB on (net) nominal interest rates but it is set at a level other than zero. What is important in both cases is that there is a lower bound that becomes binding.

[2] In the earlier version of the paper, namely, Lepetuyk et al. (2017), we solved bToTEM by using unsupervised learning (clustering) for constructing the solution domain but we use the conventional polynomial functions for approximation. In the present version, we add deep learning, namely, we replace

dimensionality. Our computational strategy differs from the conventional solution methods in three main respects. First, we introduce deep learning analysis into projection methods for analyzing dynamic economic models. Second, we combine supervised and unsupervised learning techniques into an effective computational strategy. Finally, we show how the new solution method can be used for analyzing large-scale, central banking models that are intractable up to now. There are other prominent recent papers on deep learning that had appeared while we were working on the present paper, including Duarte (2018), Villa and Valaitis (2019), Fernández-Villaverde et al. (2019), Maliar et al. (2019), and Azinović et al. (2019). We explain the relation of our work to that literature after we present our DL method.

The rest of the paper is organized as follows: In Section 2, we construct the bToTEM model. In Section 3, we describe the implementation of DL nonlinear solution methods. In Section 4, we use the bToTEM model to analyze the Canadian ELB episode. In Section 5, we assess the role of different types of nonlinearities in the bToTEM dynamics, in particular, we simulate a hypothetical increase of the inflation target from 2 to 3 percent and we analyze the role of the closing condition. Finally, in Section 6, we conclude.

2. The bToTEM model

Nowadays, the central banks, leading international organizations and government agencies, use large-scale macroeconomic models for projection and policy analysis. The term of trade economic model (ToTEM) of the Bank of Canada is among the largest: it contains 356 equations and unknowns, including 215 state variables. It includes several types of utility-maximizing consumers, several profit-maximizing production sectors, fiscal and monetary authorities, as well as a foreign sector.

At this moment, it is technically infeasible for us to solve the full-scale ToTEM nonlinearly. We therefore construct and analyze bToTEM – a scaled down version of ToTEM that has 49 equations and unknowns, including 21 state variables. In our construction of bToTEM, we follow ToTEM as closely as possible. Like the full-scale ToTEM model, the bToTEM is a small open-economy model that features the new-Keynesian Phillips curves for consumption, labor and imports. As in ToTEM, we assume the rule-of-thumb price settlers in line with Galí and Gertler (1999). We use a quadratic adjustment cost of investment and a convex cost of capital utilization. We maintain the ToTEM's terms of trade assumption, namely, we allow for bidirectional trade that consists of exporting domestic consumption goods and commodities, and importing foreign goods for domestic production. In the main text, we describe the key model's equations of bToTEM; the derivation of equilibrium conditions and extended list of the model's equations are provided in Appendix A and Appendix C, respectively. In Appendix E, we show that bToTEM produces impulse response functions that are remarkably close to those produced by ToTEM.

2.1. Production of final goods

The production sector of the economy consists of two stages. In the first stage, intermediate goods are produced by identical perfectly competitive firms from labor, capital, commodities, and imports. In the second stage, a variety of final goods are produced by monopolistically competitive firms from the intermediate goods. The final goods are then aggregated into the final consumption good.

First stage of production.

In the first stage of production, the representative, perfectly competitive firm produces an intermediate good using the following constant elasticity of substitution (CES) technology:

$$Z_t^g = \left[\delta_l (A_t L_t)^{\frac{\sigma-1}{\sigma}} + \delta_k (u_t K_t)^{\frac{\sigma-1}{\sigma}} + \delta_{com}\left(COM_t^d\right)^{\frac{\sigma-1}{\sigma}} + \delta_m (M_t)^{\frac{\sigma-1}{\sigma}}\right]^{\frac{\sigma}{\sigma-1}}, \tag{1}$$

where L_t, K_t, and COM_t^d are labor, capital and commodity inputs, respectively, M_t is imports, u_t is capital utilization, and A_t is the level of labor-augmenting technology that follows a stochastic process given by

$$\log A_t = \varphi_a \log A_{t-1} + (1-\varphi_a)\log \bar{A} + \xi_t^a, \tag{2}$$

with ξ_t^a being a normally distributed variable, and φ_a being an autocorrelation coefficient.

Capital depreciates according to the following law of motion:

$$K_{t+1} = (1-d_t)K_t + I_t, \tag{3}$$

where d_t is the depreciation rate, and I_t is investment. The depreciation rate increases with capital utilization as follows:

$$d_t = d_0 + \overline{d} e^{\rho(u_t - 1)}. \tag{4}$$

The firm incurs a quadratic adjustment cost when adjusting the level of investment. The net output is given by

$$Z_t^n = Z_t^g - \frac{\chi_i}{2}\left(\frac{I_t}{I_{t-1}} - 1\right)^2 I_t. \tag{5}$$

---

the polynomial functions with more flexible deep neural networks. This modification allowed us to increase accuracy and enhance convergence under empirically relevant parameterizations.

The objective of the firm is to choose L_t, K_{t+1}, I_t, COM_t, M_t, u_t in order to maximize profits

$$E_0 \sum_{t=0}^{\infty} \mathcal{R}_{0,t} \left(P_t^z Z_t^n - W_t L_t - P_t^i I_t - P_t^{com} COM_t^d - P_t^m M_t \right)$$

subject to (1)–(5). The firm discounts nominal payoffs according to household's stochastic discount factor $\mathcal{R}_{t,t+j} = \beta^j \left(\lambda_{t+j} / \lambda_t \right) \left(P_t / P_{t+j} \right)$, where λ_t is household's marginal utility of consumption and P_t is the final good price.

Second stage of production.

In the second stage of production, a continuum of monopolistically competitive firms indexed by i produce differentiated goods from the intermediate goods and manufactured inputs. The production technology features perfect complementarity

$$Z_{it} = \min \left(\frac{Z_{it}^n}{1 - s_m}, \frac{Z_{it}^{mi}}{s_m} \right),$$

where Z_{it}^n is an intermediate good and Z_{it}^{mi} is a manufactured input, and s_m is a Leontief parameter. The differentiated goods Z_{it} are aggregated into the final good Z_t according to the following CES technology:

$$Z_t = \left(\int_0^1 Z_{it}^{\frac{\varepsilon - 1}{\varepsilon}} di \right)^{\frac{\varepsilon}{\varepsilon - 1}}.$$

Cost minimization implies the following demand function for a differentiated good i:

$$Z_{it} = \left(\frac{P_{it}}{P_t} \right)^{-\varepsilon} Z_t, \tag{6}$$

where

$$P_t = \left(\int_0^1 P_{it}^{1-\varepsilon} di \right)^{\frac{1}{1-\varepsilon}}. \tag{7}$$

The final good is used as the manufactured inputs by each of the monopolistically competitive firms.

There are monopolistically competitive firms of two types: rule-of-thumb firms of measure ω and forward-looking firms of measure $1 - \omega$. Within each type with probability θ the firms index their price to the inflation target $\bar{\pi}_t$ as follows: $P_{it} = \bar{\pi}_t P_{i,t-1}$. With probability $1 - \theta$, the rule-of-thumb firms partially index their price to lagged inflation and target inflation according to the following rule:

$$P_{it} = (\pi_{t-1})^{\gamma} (\bar{\pi}_t)^{1-\gamma} P_{i,t-1}. \tag{8}$$

The forward-looking firms with probability $1 - \theta$ choose their price P_t^* in order to maximize profits generated when the price remains effective

$$\max_{P_t^*} E_t \sum_{j=0}^{\infty} \theta^j \mathcal{R}_{t,t+j} \left(\prod_{k=1}^{j} \bar{\pi}_{t+k} P_t^* Z_{i,t+j} - (1 - s_m) P_{t+j}^z Z_{i,t+j} - s_m P_{t+j} Z_{i,t+j} \right) \tag{9}$$

subject to demand constraints

$$Z_{i,t+j} = \left(\frac{\prod_{k=1}^{j} \bar{\pi}_{t+k} P_t^*}{P_{t+j}} \right)^{-\varepsilon} Z_{t+j}. \tag{10}$$

As in ToTEM, the presence of the rule-of-thumb firms ameliorates the forward guidance puzzle by increasing the discount on future marginal costs in the Phillips curve.

Relation between the first and second stages of production.

The production in the first and second stages are related as follows:

$$Z_t^n = \int_0^1 Z_{it}^n di = (1 - s_m) \int_0^1 Z_{it} di = (1 - s_m) \int_0^1 \left(\frac{P_{it}}{P_t} \right)^{-\varepsilon} Z_t di = (1 - s_m) \Delta_t Z_t, \tag{11}$$

where $\Delta_t = \int_0^1 \left(\frac{P_{it}}{P_t} \right)^{-\varepsilon} di$ is known as *price dispersion*.

Finally, in order to maintain the relative prices of the investment goods and noncommodity exports in accordance to the national accounts, these goods are assumed to be produced from the final goods according to linear technology that implies $P_t^i = \iota_i P_t$ and $P_t^{nc} = \iota_x P_t$, where P_t^i and P_t^{nc} are the price of investment goods and noncommodity exports goods, respectively.

2.2. Commodities

The representative, perfectly competitive domestic firm produces commodities using final goods according to the following CES technology:

$$COM_t = (Z_t^{com})^{s_z}(A_t F)^{1-s_z} - \frac{\chi_{com}}{2}\left(\frac{Z_t^{com}}{Z_{t-1}^{com}} - 1\right)^2 Z_t^{com}, \tag{12}$$

where Z_t^{com} is the final good input, and F is a fixed production factor, which may be considered as land. Similarly to production of final goods, the commodity producers incur quadratic adjustment costs when they adjust the level of final good input.

The commodities are sold domestically (COM_t^d) or exported to the rest of the world (X_t^{com})

$$COM_t = COM_t^d + X_t^{com}.$$

They are sold at the world price adjusted by the nominal exchange rate as follows:

$$P_t^{com} = e_t P_t^{comf},$$

where e_t is the nominal exchange rate (i.e., domestic price of a unit of foreign currency), and P_t^{comf} is the world commodity price. In real terms, the latter price is given by

$$p_t^{com} = s_t p_t^{comf}, \tag{13}$$

where $p_t^{com} \equiv P_t^{com}/P_t$ and $p_t^{comf} \equiv P_t^{comf}/P_t^f$ are domestic and foreign relative prices of commodities, respectively, P_t^f is the foreign consumption price level, and $s_t = e_t P_t^f/P_t$ is the real exchange rate.

2.3. Imports

The final imported good M_t is bonded from intermediate imported goods according to the following technology:

$$M_t = \left(\int_0^1 M_{it}^{\frac{\varepsilon_m - 1}{\varepsilon_m}} di\right)^{\frac{\varepsilon_m}{\varepsilon_m - 1}},$$

where M_{it} is an intermediate imported good i. The demand for an intermediate imported good i is given by

$$M_{it} = \left(\frac{P_{it}^m}{P_t^m}\right)^{-\varepsilon_m} M_t,$$

where

$$P_t^m = \left(\int_0^1 \left(P_{it}^m\right)^{1-\varepsilon_m} di\right)^{\frac{1}{1-\varepsilon_m}}.$$

We assume the prices of the intermediate imported goods to be sticky in a similar way as the prices of the differentiated final goods. A measure ω_m of the importers follows the rule-of-thumb pricing, and the others are forward looking. The optimizing forward-looking importers choose the price P_t^{m*} in order to maximize profits generated when the price remains effective

$$\max_{P_t^{m*}} E_t \sum_{j=0}^{\infty} (\theta_m)^j \mathcal{R}_{t,t+j}\left(\prod_{k=1}^{j} \bar{\pi}_{t+k} P_t^{m*} M_{i,t+j} - e_{t+j} P_{t+j}^{mf} M_{i,t+j}\right)$$

subject to demand constraints

$$M_{i,t+j} = \left(\frac{\prod_{k=1}^{j} \bar{\pi}_{t+k} P_t^{m*}}{P_{t+j}^m}\right)^{-\varepsilon_m} M_{t+j},$$

where P_t^{mf} is the price of imports in the foreign currency. All intermediate importers are foreign and they face the same marginal cost given by the foreign price of imports.

2.4. Households

The representative household in the economy has the period utility function over consumption of finished goods and a variety of differentiated labor service

$$U_t = \frac{\mu}{\mu - 1}\left(C_t - \xi \bar{C}_{t-1}\right)^{\frac{\mu-1}{\mu}} \exp\left(\frac{\eta(1-\mu)}{\mu(1+\eta)} \int_0^1 (L_{ht})^{\frac{\eta+1}{\eta}} dh\right) \eta_t^c, \tag{14}$$

where C_t is the household consumption of finished goods; $\bar{C}_t$ is the aggregate consumption, which the representative household takes as given; L_{ht} is labor service of type h; η_t^c is a consumption demand shock that follows a process

$$\log \eta_t^c = \varphi_c \log \eta_{t-1}^c + \xi_t^c, \tag{15}$$

with ξ_t^c being a normally distributed variable, and φ_c being an autocorrelation coefficient.

The representative household of type h maximizes the lifetime utility

$$E_0 \sum_{t=0}^{\infty} \beta^t U_t \tag{16}$$

subject to the following budget constraints:

$$P_t C_t + \frac{B_t}{R_t} + \frac{e_t B_t^f}{R_t^f\left(1+\kappa_t^f\right)} = B_{t-1} + e_t B_{t-1}^f + \int_0^1 W_{ht} L_{ht} dh + \Pi_t, \tag{17}$$

where B_t and B_t^f are holdings of domestic and foreign-currency denominated bonds, respectively; R_t and R_t^f are domestic and foreign nominal interest rate, respectively; κ_t^f is the risk premium on the foreign interest rate; W_{ht} is the nominal wage of labor of type h; Π_t is profits paid by the firms.

2.5. Wage setting

The representative household supplies a variety of differentiated labor service to the labor market, which is monopolistically competitive. The differentiated labor service is aggregated according to the following aggregation function:

$$L_t = \left(\int_0^1 L_{ht}^{\frac{\varepsilon_w - 1}{\varepsilon_w}} dh\right)^{\frac{\varepsilon_w}{\varepsilon_w - 1}}.$$

Aggregated labor L_t is demanded by firms in the first stage of production. A cost minimization of the aggregating firm implies the following demand for individual labor:

$$L_{ht} = \left(\frac{W_{ht}}{W_t}\right)^{-\varepsilon_w} L_t, \tag{18}$$

where W_{ht} is wage for labor service of type h, and W_t is defined by the following:

$$W_t \equiv \left(\int_0^1 W_{ht}^{1-\varepsilon_w} dh\right)^{\frac{1}{1-\varepsilon_w}}. \tag{19}$$

Wages are set by labor unions that are of two types: rule-of-thumb unions of measure ω_w and forward-looking unions of measure $1-\omega_w$. Within each type, with probability θ_w the labor unions index their wage to the inflation target $\bar{\pi}_t$ as follows $W_{it} = \bar{\pi} W_{i,t-1}$. The rule-of-thumb unions that do not index their wage in the current period follow the rule

$$W_{it} = \left(\pi_{t-1}^w\right)^{\gamma_w} (\bar{\pi}_t)^{1-\gamma_w} W_{i,t-1}. \tag{20}$$

The forward-looking unions that do not index their wage choose the wage W_t^* optimally in order to maximize the household utility function when the wage for their type is effective

$$E_t \sum_{j=0}^{\infty} (\beta\theta_w)^j U_{t+j} \tag{21}$$

subject to labor demand (18) written as

$$L_{h,t+j} = \left(\frac{\prod_{k=1}^{j} \bar{\pi}_{t+k} W_t^*}{W_{t+j}}\right)^{-\varepsilon_w} L_{t+j}, \tag{22}$$

and budget constraints (17) which can be written as

$$P_{t+j} C_{t+j} = \prod_{k=1}^{j} \bar{\pi}_{t+k} W_t^* L_{h,t+j} dh + \Psi_{t+j},$$

where Ψ_{t+j} includes terms other than C_{t+j} and $L_{h,t+j}$.

2.6. Monetary policy

The monetary authority sets the short-term nominal interest rate in response to a deviation of the actual inflation rate from the target and a deviation of the actual output from potential output,

$$\Phi_t = \rho_r R_{t-1} + (1-\rho_r)\left[\bar{R} + \rho_\pi(\pi_t - \bar{\pi}_t) + \rho_Y\left(\log Y_t - \log \bar{Y}_t\right)\right] + \eta_t^r, \tag{23}$$

where ρ_r measures the degree of smoothing of the interest rate; $\bar{R}$ is the long-run nominal interest rate; ρ_π measures a long-run response to the inflation gap; $\bar{\pi}_t$ is the inflation target; ρ_Y measures a long-run response to the output gap; $\bar{Y}_t$ is the potential level of output; η_t^r is an interest rate shock that is assumed to follow the following process:

$$\eta_t^r = \varphi_r \eta_{t-1}^r + \xi_t^r,$$

where ξ_t^r is a normally distributed variable, and φ_r is an autocorrelation coefficient. Potential output changes with productivity in the following stylized way:

$$\log \bar{Y}_t = \varphi_z \log \bar{Y}_{t-1} + (1-\varphi_z)\log\left(\frac{A_t \bar{Y}}{\bar{A}}\right).$$

If an effective lower bound R_t^{elb} is imposed on the nominal interest rate, the interest rate is determined as a maximum of (23) and R_t^{elb}:

$$R_t = \max\left\{R_t^{elb}, \Phi_t\right\}.$$

2.7. Foreign demand for noncommodity exports

We assume that the foreign demand for noncommodity exports is given by the following demand function:

$$X_t^{nc} = \gamma^f \left(\frac{P_t^{nc}}{e_t P_t^f}\right)^{-\phi} Z_t^f, \tag{24}$$

where P_t^{nc} is a domestic price of noncommodity exports and Z_t^f is a foreign activity measure. In real terms, we have

$$X_t^{nc} = \gamma^f \left(\frac{s_t}{p_t^{nc}}\right)^{\phi} Z_t^f. \tag{25}$$

2.8. Balance of payments

The balance of payments is

$$\frac{e_t B_t^f}{R_t^f\left(1+\kappa_t^f\right)} - e_t B_{t-1}^f = P_t^{nc} X_t^{nc} + P_t^{com} X_t^{com} - P_t^m M_t, \tag{26}$$

where B_t^f is domestic holdings of foreign-currency denominated bonds, and R_t^f is the nominal interest rate on the bonds. In real terms, it becomes

$$\frac{b_t^f}{r_t^f\left(1+\kappa_t^f\right)} - b_{t-1}^f \frac{s_t}{s_{t-1}} = \frac{1}{\bar{Y}}\left(p_t^{nc} X_t^{nc} + p_t^{com} X_t^{com} - p_t^m M_t\right), \tag{27}$$

where the bond holdings are normalized as $b_t^f = \frac{s_t B_t^f}{P_{t+1}^f \bar{Y}}$, and r_t^f is the real interest rate on the foreign-currency denominated bonds.

2.9. Rest-of-the-world economy

The rest of the world is specified by three exogenous processes that describe the evolution of foreign variables. First, the evolution of the foreign activity measure Z_t^f is given by

$$\log Z_t^f = \varphi_{zf} \log Z_{t-1}^f + \left(1-\varphi_{zf}\right)\log \bar{Z}^f + \xi_t^{zf}, \tag{28}$$

second, the foreign real interest rate r_t^f follows

$$\log r_t^f = \varphi_{rf} \log r_{t-1}^f + \left(1-\varphi_{rf}\right)\log \bar{r} + \xi_t^{rf}, \tag{29}$$

finally, a foreign commodity price p_t^{comf} is

$$\log p_t^{comf} = \varphi_{comf} \log p_{t-1}^{comf} + \left(1-\varphi_{comf}\right)\log \bar{p}^{comf} + \xi_t^{comf}, \tag{30}$$

where ξ_t^{zf}, ξ_t^{rf} and ξ_t^{comf} are normally distributed random variables, and φ_{Zf}, φ_{rf} and φ_{comf} are the autocorrelation coefficients.

2.10. Uncovered interest rate parity

We impose an augmented uncovered interest rate parity condition

$$e_t = E_t\left[(e_{t-1})^{\varkappa}\left(e_{t+1}\frac{R_t^f\left(1+\kappa_t^f\right)}{R_t}\right)^{1-\varkappa}\right], \tag{31}$$

where the term $(e_{t-1})^{\varkappa}$ under the brackets is added to mimic the relationship assumed in ToTEM; see Appendix A.4 for some more details. The augmentation reduces the responsiveness of the exchange rate to a change in the interest rate differential.

2.11. Market clearing conditions

We close the model by the following resource feasibility condition:

$$Z_t = C_t + \iota_i I_t + \iota_x X_t^{nc} + Z_t^{com} + \upsilon_z Z_t. \tag{32}$$

We define GDP and GDP deflator as follows:

$$Y_t = C_t + I_t + X_t^{nc} + X_t^{com} - M_t + \upsilon_y Y_t, \tag{33}$$

$$P_t^y Y_t = P_t C_t + P_t^i I_t + P_t^{nc} X_t^{nc} + P_t^{com} X_t^{com} - P_t^m M_t + \upsilon_y P_t^y Y_t,$$

in real terms, the latter becomes

$$p_t^y Y_t = C_t + p_t^i I_t + p_t^{nc} X_t^{nc} + p_t^{com} X_t^{com} - p_t^m M_t + \upsilon_y p_t^y Y_t. \tag{34}$$

2.12. Stationarity condition for the open-economy model

The budget constraint (17) of the domestic economy contains $R_t^f\left(1+\kappa_t^f\right)$ where R_t^f is the rate of return to foreign assets and κ_t^f is the risk premium. If the rate of return to foreign assets does not depend on quantity purchased, then the domestic economy can maintain nonvanishing long-run growth by investing in foreign assets. Schmitt-Grohé and Uribe (2003) explore several alternative assumptions that make it possible to prevent this undesirable implication and to attain stationarity in open-economy models. We adopt one of their assumptions, namely, we assume that the risk premium κ_t^f is a decreasing function of foreign assets

$$\kappa_t^f = \varsigma\left(\bar{b}^f - b_t^f\right), \tag{35}$$

where $\bar{b}^f$ is the steady-state level of the normalized bond holdings. This assumption ensures a decreasing rate of return to foreign assets. As we will see, a specific functional form assumed for modeling risk premium plays an important role in the model's predictions.

2.13. Calibration of bToTEM

The bToTEM model contains 61 parameters to be calibrated. Whenever possible, we use the same values of parameters in bToTEM as those in ToTEM, and we choose the remaining parameters to reproduce a selected set of observations from the Canadian time series data. In particular, our calibration procedure targets the ratios of six nominal variables to nominal GDP $P_t^y Y_t$, namely, consumption $P_t C_t$, investment $P_t^i I_t$, noncommodity export $P_t^{nc} X_t^{nc}$, commodity export $P_t^{com} X_t^{com}$, import $P_t^m M_t$, total commodities $P_t^{com} COM_t$, and labor input $W_t L_t$. Furthermore, we calibrate the persistence of shocks so that the standard deviations of the selected bToTEM variables coincide with those of the corresponding ToTEM variables, namely, those of domestic nominal interest rate R_t, productivity A_t, foreign demand Z_t^f, foreign commodity price p_t^{comf}, and foreign interest rate r_t^f. The parameters choice is summarized in Tables D.1 and D.2 provided in Appendix D.

3. A deep-learning global solution method

bToTEM is a complex nonlinear model that represents a serious challenge to the existing global nonlinear solutions methods. First, bToTEM has much higher dimensionality – 21 state variables – than the new Keynesian models studied in the literature with the global solution methods. Second, the open-economy bToTEM model produces a more complex system of equations than a baseline closed-economy new Keynesian model studied nonlinearly in the literature, namely, bToTEM has more than 30 nonlinear equations that must be treated with a numerical solver in all grid points, as well as in all future states, inside the main iterative loop. Finally, the economy faces an occasionally binding ELB constraint on the nominal interest rate.

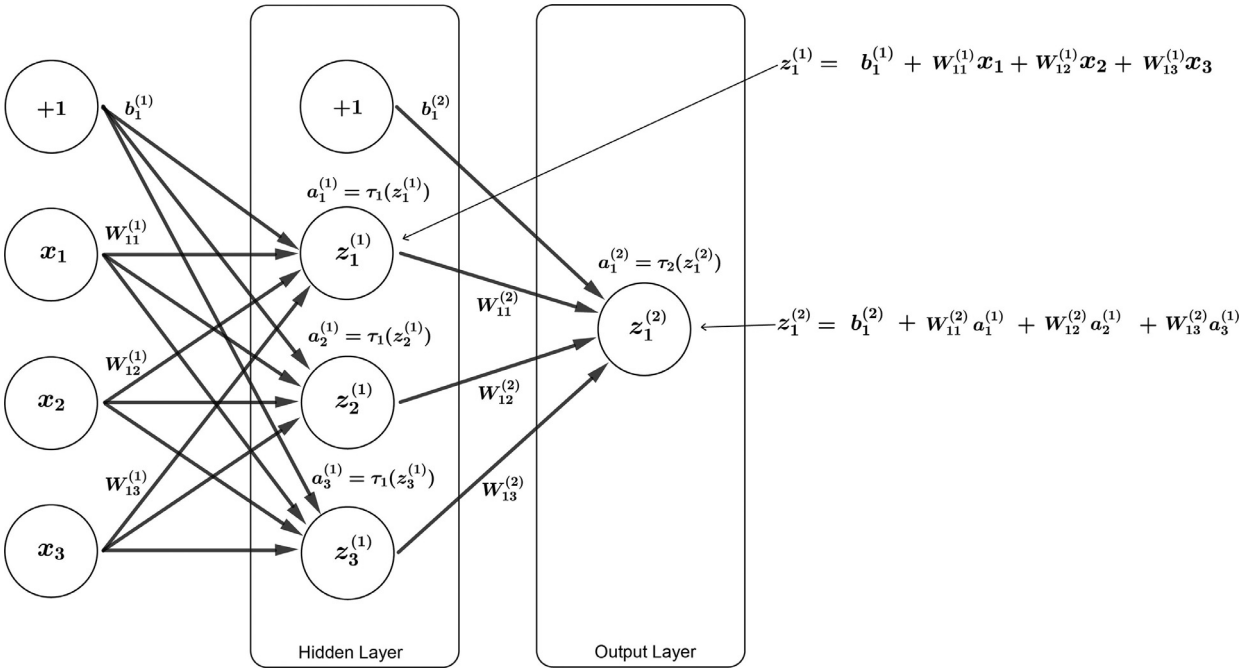

Fig. 1. Three layer neural network

To address the challenges of bToTEM, we introduce a deep learning (DL) projection method that relies on a combination of supervised and unsupervised learning techniques. Specifically, we use a multilayer neural network for approximating decision functions, and we use simulation and clustering analysis for constructing the solution domain. In this section, we describe these techniques, explain how they help us deal with the curse of dimensionality and discuss the relation of our DL method to the literature.

3.1. Supervised learning: deep neural network

Deep neural networks are a flexible parametric family of functions which can be used as an alternative to traditional approximating functions such as polynomials or splines, in particular, in high-dimensional applications. In Fig. 1, we show a three-layer neural network that we use for constructing the solution to bToTEM; such a network consists of three layers – one input, one hidden and one output layers; in the figure, layers are represented by superscripts. The input layer consists of a vector of inputs $x \in \mathbb{R}^n$ to which we add a constant term of one, denoted as "+1" in the figure. In both hidden and output layers, we first construct a linear combination of inputs, called the "nonactivated neuron" $z \equiv b + Wx$, where b is a bias that corresponds to the constant term, and $W \in \mathbb{R}^n$ is a vector of weights that corresponds to the vector of inputs x. We then transform the nonactivated neuron z into activated neuron a using an activation function $a = \tau(z)$.

In the hidden layer, as an activation function, we use a symmetric sigmoid function, namely, the hyperbolic tangent function $\tanh(z) = 2/[1 + \exp(-2z)] - 1$. Thus, each activated neuron i of the hidden layer is constructed by applying the same activation function to inputs

$$a_i^{(1)} = \tau_1\left(z_i^{(1)}\right) = \tanh\left(b_i^{(1)} + W_i^{(1)}x\right),$$

however it has its own bias $b_i^{(1)}$ and a vector of weights $W_i^{(1)}$.

In the output layer, as an activation function, we use a simple identity function $\tau(z) = z$, so activated and nonactivated neurons coincide. The inputs of this layer are the activated neurons of the hidden layer $a^{(1)}$ to which we also add the constant term. Thus, each output i of the output layer is given by

$$y_i = z_i^{(2)} = b_i^{(2)} + W_i^{(2)}a^{(1)},$$

where $b_i^{(2)}$ and $W_i^{(2)}$ are the corresponding bias and weights.

A straightforward construction of inputs for a neural network would be to use a vector of 21 state variables of bToTEM plus a constant term. However, we chose to construct a more flexible approximation by using quadratic basis (terms of the second-order ordinary polynomial) of the state variables as an input. For 21 state variables of bToTEM, the quadratic base consist of 252 variables plus the constant term of one. This approach allows us to reduce the degree of nonlinearity explicitly attributed to the neural network and to achieve higher accuracy with just one hidden layer. The quadratic basis also helps

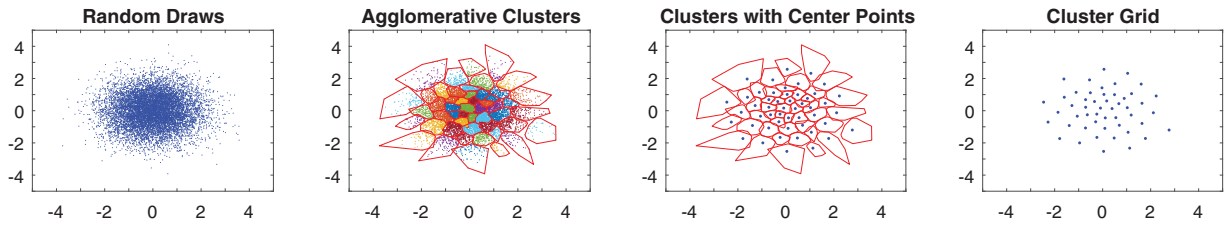

Fig. 2. Construction of a cluster grid from simulated points

us facilitate convergence of the iterative fixed-point algorithm that we used to compute the coefficients and weights of the neural network.

We use 11 neurons in both hidden and output network layers to match the number of bToTEM intertemporal choice variables. For this number of neurons, the neutral network includes 2,915 coefficients: there are 2,783 coefficients in the hidden layer, and there are 132 coefficients in the output layer. All inputs and outputs of the neural network are normalized by a linear transformation to lie within an interval $[-1, 1]$.

3.2. Unsupervised learning: clustering analysis

We construct the solution to be accurate in the high-probability area of the state space, instead of focusing on a much larger conventional rectangular domain. To produce a grid in the high-probability area of the state space, we use cluster grid analysis (CGA); see Maliar et al. (2011), and Maliar and Maliar (2015) for a discussion of this and other ergodic-set techniques. Our grid construction can be understood by looking at a two-dimensional example in Fig. 2.

In the first panel of the figure, we see a cloud of points that is obtained by stochastic simulation of an economic model: this cloud covers a high-probability area of the state space. The crude simulated cloud contains many redundant points that are located close to one another. The CGA method eliminates the redundancy by replacing a large set of simulated points with a smaller set of "representative" points. This process is illustrated in the remaining panels of the figure: first, CGA splits the simulated points into a set of clusters; then it computes the centers of the clusters; and finally, it uses the centers of the clusters as a grid for constructing a nonlinear solution. To measure the distance between simulated points, we compute the principal components of the simulated data and we normalize them to unit standard deviation. To distinguish clusters, we use a hierarchical clustering algorithm with the Euclidean distance and Ward linkage. Finally, to construct the centers, we compute simple averages of all simulated points that belong to the clusters distinguished.

3.3. Implementation details of the DL solution method

For the purpose of constructing nonlinear global solutions, we split the variables of the bToTEM model into four types (see Appendix B for the list of model variables):

- exogenous state variables,

$$\mathbf{Z}_t \equiv \left\{A_t, \eta_t^R, \eta_t^c, p_t^{comf}, r_t^f, Z_t^f\right\},$$

- endogenous state variables,

$$\mathbf{S}_t \equiv \left\{C_{t-1}, R_{t-1}, s_{t-1}, \pi_{t-1}, \Delta_{t-1}, w_{t-1}, \pi_{t-1}^w, \Delta_{t-1}^w, p_{t-1}^m, \pi_{t-1}^m, I_{t-1}, Z_{t-1}^{com}, b_{t-1}^f, \bar{Y}_{t-1}, K_{t-1}\right\},$$

- endogenous intertemporal choice variables; these are variables that enter the model equations at both t and $t+1$, where a $t+1$ value is a random variable unknown at t,

$$\mathbf{Y}_t \equiv \left\{F_{1t}, F_{2t}, F_{1t}^w, F_{2t}^w, F_{1t}^m, F_{2t}^m, q_t, \lambda_t, s_t, ex_t^i, ex_t^{com}\right\},$$

- endogenous intratemporal choice variables; these are variables that are determined within the current period t, given the intertemporal choice,

$$\mathbf{X}_t \equiv \left\{\begin{array}{c} L_t, K_t, I_t, COM_t^d, M_t, u_t, d_t, Z_t^g, Z_t^n, Z_t, C_t, Y_t, \pi_t, rmc_t, \Delta_t, \pi_t^m, \bar{\pi}_t, p_t^m, R_t, p_t^z, w_t, \\ MPK_t, R_t^k, p_t^i, \kappa_t^f, b_t^f, X_t^{nc}, X_t^{com}, COM_t, Z_t^{com}, \pi_t^w, w_t^*, \Delta_t^w, \bar{Y}_t, p_t^{com}, p_t^{nc}, p_t^{mf}, p_t^y \end{array}\right\}.$$

The DL method is implemented in the context of the bToTEM model as summarized in Algorithm 1.

To compute conditional expectations in the intertemporal choice conditions, we use a monomial formula with $2N$ nodes, where $N = 6$ is the number of stochastic shocks; see Maliar and Maliar (2014) for a description of this formula. To solve for intratemporal choice variables $\mathbf{X}_m'$, we use a numerical solver. As for the intratemporal choice variables in the integration nodes $\mathbf{X}_{m,j}'$, we find them either with a numerical solver or by using interpolation of the intratemporal choice decision function $\mathbf{X}_m'$ constructed for the current period using a numerical solver. We rely on Levenberg-Marquardt optimization to train the neural network in order to update the neural network coefficients $\widehat{\mathbf{v}}_Y$. Following the common practice in the deep

Algorithm 1 A global nonlinear DL solution method

Step 0. Initialization

a. Choose simulation length T and fix initial conditions $\mathbf{Z}_0 \equiv \left\{A_0, \eta_0^R, \eta_0^c, p_0^{comf}, r_0^f, Z_0^f\right\}$ and $\mathbf{S}_0$.

b. Draw $\left\{\xi_{t+1}^A, \xi_{t+1}^R, \xi_{t+1}^c, \xi_{t+1}^{comf}, \xi_{t+1}^{rf}, \xi_{t+1}^{Zf}\right\}_{t=0}^{T-1}$ and construct $\mathbf{Z}_t \equiv \left\{A_t, \eta_t^R, \eta_t^c, p_t^{comf}, r_t^f, Z_t^f\right\}_{t=0}^{T}$.

c. Construct perturbation decision functions $\widehat{\mathbf{Z}}(\cdot; \mathbf{b}_Z)$, $\widehat{\mathbf{S}}(\cdot; \mathbf{b}_S)$, $\widehat{\mathbf{Y}}(\cdot; \mathbf{b}_Y)$ and $\widehat{\mathbf{X}}(\cdot; \mathbf{b}_X)$, where $\mathbf{b}_Z$, $\mathbf{b}_S$, $\mathbf{b}_Y$ and $\mathbf{b}_X$ are the polynomial coefficients.

d. Use the perturbation solution to produce simulation $\{\mathbf{Y}_t, \mathbf{X}_t, \mathbf{S}_t, \mathbf{Z}_t\}_{t=0}^T$ of $T+1$ observations.

e. Construct a grid for endogenous and exogenous state variables $\{\mathbf{S}_m, \mathbf{Z}_m\}_{m=1,...,M}$ by using agglomerative clustering analysis.

f. Choose approximating functions (neural networks) for parameterizing the intertemporal choice: $\mathbf{Y}_t \approx \widehat{\mathbf{Y}}(\cdot; \mathbf{v}_Y)$, where $\mathbf{v}_Y$ is the parameter vector for the global solution method.

g. Use the perturbation solution $\widehat{\mathbf{Y}}(\cdot; \mathbf{b}_Y)$ to construct an initial guess on $\mathbf{v}_Y$.

h. Choose integration nodes, $\left\{\xi_j^A, \xi_j^R, \xi_j^c, \xi_j^{comf}, \xi_j^{rf}, \xi_j^{Zf}\right\}_{j=1,...,J}$ and weights, $\left\{\omega_j\right\}_{j=1,...,J}$.

i. Compute and fix future exogenous states $\mathbf{Z}'_{m,j} \equiv \left\{A_{m,j}, \eta_{m,j}^R, \eta_{m,j}^c, p_{m,j}^{comf}, r_{m,j}^f, Z_{m,j}^f\right\}_{m=1,...,M}$.

Step 1. Updating the intertemporal decision functions

At iteration i, for $m = 1, ..., M$,

a. Compute intertemporal choice variables $\mathbf{Y}'_m \approx \widehat{\mathbf{Y}}(\mathbf{S}_m, \mathbf{Z}_m; \mathbf{v}_Y)$.

b. Compute intratemporal choice variables $\mathbf{X}'_m$ satisfying the intratemporal choice equations.

c. Form $\mathbf{S}'_m$ from $\mathbf{Y}'_m$ and $\mathbf{X}'_m$.

d. Compute intertemporal choice variables in J integration nodes $\mathbf{Y}'_{m,j} \approx \widehat{\mathbf{Y}}\left(\mathbf{S}'_m, \mathbf{Z}'_{m,j}; \mathbf{v}_Y\right)$.

e. Compute intratemporal choice variables $\mathbf{X}'_{m,j}$ in J satisfying the intratemporal choice equations.

f. Substitute the results in the intertemporal choice equations and compute $\widehat{\mathbf{Y}}_m$.

g. Find $\mathbf{v}$ that minimizes the distance $\widehat{\mathbf{v}}_Y \equiv \arg\min_{\mathbf{v}} \sum_{m=1}^M \left\|\widehat{\mathbf{Y}}_m - \widehat{\mathbf{Y}}(\mathbf{S}_m, \mathbf{Z}_m; \mathbf{v})\right\|$.

h. Use damping to compute $\mathbf{v}_Y^{(i+1)} = (1-\lambda)\mathbf{v}_Y^{(i)} + \lambda\widehat{\mathbf{v}}_Y$, where $\lambda \in (0, 1)$ is a damping parameter.

i. Check for convergence and end iteration if $\frac{1}{M}\max \sum_{m=1}^{M} \left|\frac{\mathbf{Y}_m^{(i+1)} - \mathbf{Y}_m^{(i)}}{\mathbf{Y}_m^{(i)}}\right| < \varpi$.

Proceed to the next iteration and iterate on these steps until convergence.

learning literature, we do not use all the data (grid points) for training but we split them into training, validation and testing samples in the proportion 70, 15 and 15 percent, respectively. In each iteration, we alternate the training and validation steps until the appropriate regularization hyperparameter is computed. The testing sample was used both to monitor the quality of approximation in each iteration and to determine the number of epochs (iterations) necessary for convergence of our approximations. The damping parameter is set at $\lambda = 0.1$, and the convergence criterion is set at $\varpi = 10^{-7}$. The running time for constructing our global DL solution was about 6 hours;[3] the running time is sensitive to a specific choice of the damping parameter λ.

3.4. Designing the DL method to address the challenges of bToTEM

How does our design of the DL method help us address the challenges of bToTEM? First of all, the introduction of neural networks was critical for producing accurate solutions. To be specific, in the earlier version of the present paper, namely, Lepetuyk et al. (2017), we approximated the decision functions by using the conventional polynomial functions. However, such function were not flexible enough for accurate approximations, and our method ran into the problem of non-convergence. To attain convergence, we scaled down the volatility of shocks, which also reduced the role of nonlinearities in the earlier version. In the current version, we both increased accuracy and enhanced convergence by replacing polynomials with deep neural networks. Our current DL algorithm is capable of constructing an accurate global nonlinear solution under empirically relevant volatility of shocks. As a result, the effects of nonlinearities on the solution became more important. However, the improvements came at a cost: the introduction of deep neural networks instead of polynomial functions increased the running time up to 10 times. In turn, the cluster grid technique was critical for making our DL method tractable. This technique reduces computational expenses in three ways. First, it allows us to restrict attention only to the ergodic area in which the solution "lives", which is typically an infinitesimally small fraction of the high-dimensional hypercube domain used by conventional projection methods; see Maliar and Maliar (2014) for a discussion. Second,

[3] Our hardware is Intel® Core™ i7-2600 CPU @ 3.400 GHz with RAM 12.0 GB. Our software is written and executed in MATLAB 2019a. We parallelize the computation across four cores.

clustering reduces the number of grid points compared to pure simulation method, such as parameterized expectation algorithm in Den Haan and Marcet (1990), Duffy and McNelis (2001) and Villa and Valaitis (2019). Given that the system of the bToTEM equations is treated with an expensive numerical solver in each grid point and integration node, the reduction in the number of grid points by clustering reduces the cost dramatically. Finally, it avoids the need to re-simulate grid points in each iteration, namely, we construct the grid just once in the beginning of the solution procedure using some low-accuracy solution such as a first-order perturbation solution. (We checked that updating the grid as the solution refines does not practically affect accuracy in our model).

Re-simulating the solution along iteration is an indispensable step of a pure simulation but not projection methods. This is because the simulation methods use simulated points for constructing expectation functions. If such simulation points are produced by a low-accuracy solution, the expectation functions are computed inaccurately, which leads to the low overall accuracy of solutions. This is not the case for our projection method that uses simulated points only for constructing the grid but computes expectation functions using an accurate monomial integration method; see Maliar and Maliar (2014) for a survey of this and other deterministic integration methods. For smooth functions like bToTEM decision functions, the monomial rules are remarkably accurate with just few integration nodes, while Monte-Carlo integration methods have a low square-root rate of convergence and thus require long simulation for accurate solutions; see Maliar and Maliar (2014) for a comparison analysis. Finally, to compute the fixed-point parameters of the neural network, we use derivative-free fixed-point iteration. Taken together, the above techniques make our DL method tractable in problems with high dimensionality like bToTEM!

3.5. Relation to the literature

The key novel feature of our solution method is the use of DL techniques for approximating decision functions which we introduce following the recent trends in computer-science literature; see Goodfellow et al. (2016). The application of neural networks in economic dynamics is dated back to a seminal work of Duffy and McNelis (2001) who incorporated this functional family into the parameterized expectation algorithm of Den Haan and Marcet (1990).

The subsequent progress in that direction was slow, however, recently, several papers applied deep learning methods to analyze their dynamic economic models. In particular, Duarte (2018) and Fernández-Villaverde et al. (2019) use neural networks in the context of continuous-time models, specifically, the former paper uses neural networks to construct a solution to the Bellman equation in the optimal control problems in finance, and the latter paper uses neural networks for approximating a nonlinear aggregate law of motion in a version of Krusell and Smith (1998) model. In a discrete-time application, Villa and Valaitis (2019) show that neural networks can help to deal with ill-conditioning in the context of the parameterized expectation algorithm. Our DL analysis shares the use of simulation techniques with the latter paper, however, we incorporate additional projection-style elements such as clustering and deterministic integration that lead to important advantages over pure simulation methods; see our discussion in Section 3.4.

Furthermore, Maliar et al. (2018) introduce a different DL approach that allows to cast the entire economic model (in the form of lifetime reward and residuals in the Euler and Bellman equations) into an objective function of supervised learning which is optimized via the Google TensorFlow platform. This approach is developed further in Maliar et al. (2019) who solve Krusell and Smith (1998) model using the model-reduction property of neural networks instead of relying on approximate aggregation. Finally, Azinović et al. (2019) show a method similar to Maliar et al. (2018), Maliar et al. (2019) and they use it to solve a life-cycle model. The key difference of the DL analysis from the above literature is that the literature focuses on supervised (deep) learning techniques for approximation of decision functions via Monte Carlo simulation, while the present paper emphasizes benefits of combining supervised and unsupervised learning methods into an effective DL computational strategy for analyzing high-dimensional applications.

4. Was the Canadian ELB crisis imported from abroad?

In the U.S. and European countries, the Great Recession and the ELB episodes were caused by the 2008 financial crisis. In contrast, Canada did not experience any significant financial crisis or economic slowdown at the beginning of the Great Recession. Nonetheless, Canada also ended up reaching ELB on nominal interest rates and remained there during the 2009–2010 period. To be specific, the Bank of Canada targeted the overnight interest rate at 0.25 percent annually, which at that time was viewed by the Bank of Canada to be a lower bound on the nominal interest rate.

What factors led the Canadian economy to the ELB crisis? In this section, we argue that the recession spread to Canada from the rest of the world, primarily from the U.S., which is the main Canadian trade partner (around 75 percent of Canadian exports go to the U.S.). The Canadian economy experienced a huge (16 percent over 3 quarters) drop in exports in the beginning of the Great Recession; see a speech by Boivin (2011), a former Deputy Governor of the Bank of Canada. Using bToTEM simulation, we find that negative foreign shocks of such magnitude are sufficient to produce a prolonged ELB episode in the Canadian economy.

4.1. Generating the ELB episode in Canada using foreign shocks

Calibration of exogenous foreign shocks using ToTEM.

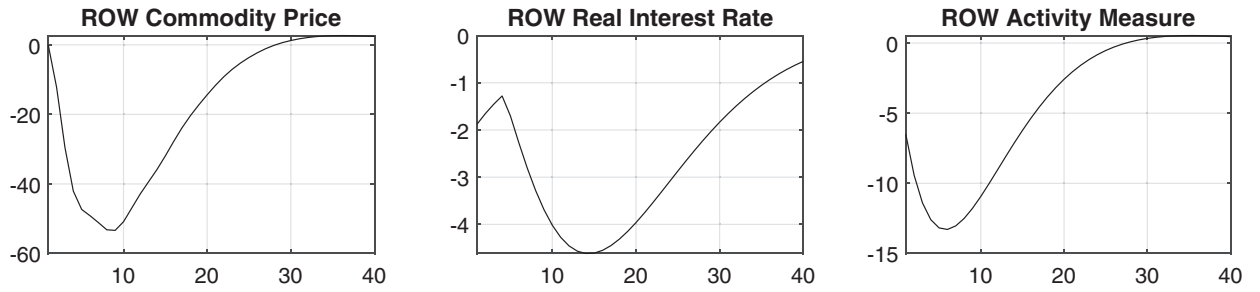

Fig. 3. Exogenous ROW shocks

An important question is how to realistically calibrate the behavior of the rest of the world (ROW) sector in the bToTEM model since foreign financial crisis affects not just foreign demand but also foreign prices and foreign interest rates. Our methodology combines the analysis of bToTEM and ToTEM. Namely, we first simulate ToTEM to produce impulse responses to a negative ROW shock, and we then fed the resulting responses into bToTEM as exogenous state variables. The ROW sector in ToTEM consists of three variables: a ROW interest rate, a ROW commodity price and a ROW activity measure. These three shocks produced by ToTEM are shown in Fig. 3.

A negative shock in the ROW sector has three effects in ToTEM: first, the ROW commodity price reduces (because the world demand goes down); second, the ROW nominal interest rate reduces (since the monetary authority in the ROW model is assumed to follow a Taylor rule); and third, the foreign activity measure declines (because the ROW foreign demand decreases). The size of the ROW shocks generated by ToTEM is in line with the data. Specifically, the ROW commodity price shock in the figure matches a 50 percent decline in the global commodity price index documented by the IMF.[4] The ROW real interest rate shock matches a 5 percent peak-to-trough decline in the effective U.S. federal funds rate.[5] The ROW activity measure shock is slightly smaller than an 18 percent decline in the foreign activity measure estimated by the Bank of Canada.[6] See also another related observation of a 20 percent peak-to-trough decline of Canadian exports during the Great Recession. When we fed the ROW shocks from ToTEM into bToTEM, we obtain an ELB episode that is similar to the one observed in the Canadian data.

bToTEM simulation of the ELB episode in Canada.

Fig. 4 displays the simulated time series for the key model variables under the given behavior of the ROW sector imported from ToTEM. Here, ELB on the nominal interest rate is set at 2 percentage points below the deterministic steady state of the nominal interest rate. All the variables are reported in percentage deviations from the deterministic steady state, except of inflation and the interest rates that are shown in annualized deviations from the deterministic steady state. We assume that initially, the domestic interest rate in bToTEM is slightly below the deterministic steady state, namely, by 1 percent, which makes it is easier to reach ELB on the nominal interest rate.[7]

We plot three different solutions, namely, a first-order perturbation solution with ELB imposed; a plain second-order perturbation solution produced by Dynare without imposing ELB; and a DL solution with ELB imposed. To impose ELB on the perturbation solution, we use the IRIS toolbox by Beneš et al. (2015) that deals with occasionally binding constraints by introducing auxiliary anticipated shocks as in Laséen and Svensson (2011). We also checked that the IRIS produces the same solutions as the OccBin toolbox developed by Guerrieri and Iacoviello (2015); see also Holden (2016) for a related method. As we see, the three solutions look very similar in the figure, so we conclude that the nonlinearities do not significantly affect the solution in this particular simulation experiment.

To check the accuracy of numerical solutions, we compute unit-free residuals in the model's equation along the simulation path; see Appendix F for details of our accuracy assessment. As expected, the global solution method is the most accurate. The least accurate first-order perturbation method can produce residuals of order $10^{-1.44} \approx 3.6$ percent, while the DL method produces residuals which are about an order of magnitude lower, namely, equal to $10^{-2.37} \approx 0.4$ percent. (The accuracy results are similar on a stochastic simulation). Given that all three numerical solutions look similar, we conclude that numerical errors of these magnitudes do not affect the qualitative implications of the model in this experiment.

A modest role of nonlinearity in our baseline simulation is not a generic property of the bToTEM model but a numerical finding that is valid just for these specific simulation and calibration procedures. We could have increased the difference between linear and nonlinear solutions by augmenting volatility of shocks (still within a reasonable range) or by

[4] Source: All Commodity Price Index, incudes both Fuel and non-Fuel Price Indices. IMF Data. https://data.imf.org/

[5] Source: Effective Federal Funds Rate, https://fred.stlouisfed.org/series/FEDFUNDS

[6] Source: Foreign Activity Measure. Indicators of Capacity and Inflation Pressures for Canada. Bank of Canada. https://www.bankofcanada.ca/rates/indicators/capacity-and-inflation-pressures/product-market-definitions/product-market-historical-data/

[7] The natural yearly rate of interest in bToTEM is calibrated to 3 percent as in ToTEM. This value is chosen to represent the long-run historical average of the natural rate of interest in the Canadian economy. However, the current natural rate of interest in Canada is considerably lower. Setting the initial interest rate below the steady state is a way to account for the current low interest rate.

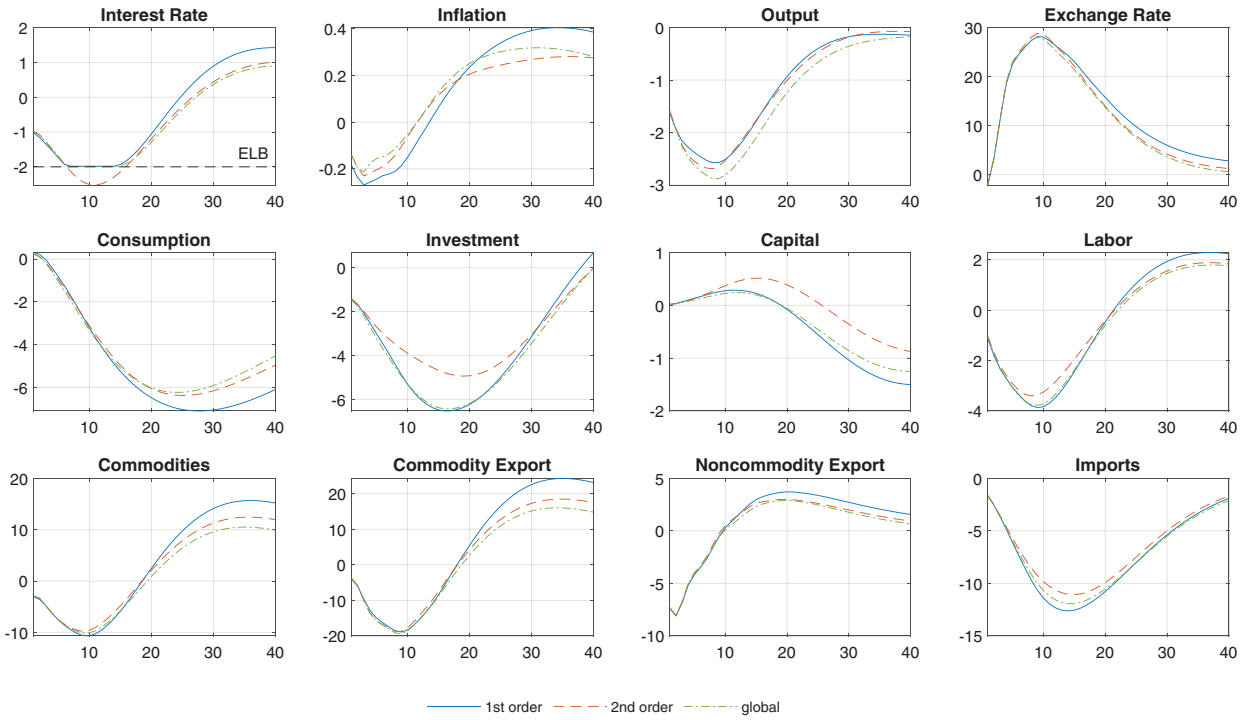

Fig. 4. Responses of linear perturbation, quadratic perturbation, and global DL solutions to ROW shocks

modifying some model's assumptions (such as the closing cost specification considered in Section 5.2). However, it was not the goal of our analysis to find parameterizations that emphasize the role of nonlinearities. Rather, our goal was to meticulously calibrate the bToTEM model to reproduce the Canadian data, trying to make it as close as possible to the full-scale ToTEM model. It turned out that under such calibration, nonlinearities proved to be relatively unimportant, including ELB. In Section 5, we show simulation experiments in which nonlinearities are important.

Understanding the ELB episode in Canada: a contagion mechanism.

Under the considered scenario of negative ROW shocks, there are three foreign variables that decline during the crisis, namely, the foreign activity measure, the foreign interest rate, and the world commodity price; see Fig. 3. The immediate consequence of these shocks for the domestic economy in Fig. 4 is a sharp decline in commodity and noncommodity exports in the Canadian economy. There are significantly fewer commodities extracted due to a huge decline in commodity prices and as a consequence, domestic output starts declining. The central bank responds by lowering the interest rate to stimulate the economy but the magnitude of shocks is so large that the bank reaches the lower bound on the nominal interest rate by six quarters. Without unconventional monetary tools, the interest rate stays at the lowest value for two years until the foreign economy sufficiently recovers. All three numerical methods considered deliver the same qualitative predictions about the ELB episode. Thus, the proposed contagion-style mechanism is strong enough to account for this ELB episode in the Canadian economy.[8]

How robust is the contagion mechanism to the key bToTEM assumptions?

To evaluate the robustness of the contagion mechanism, we conduct three sensitivity exercises. First, we consider an economy without the rule-of-thumb firms and unions. Such a model exhibits a noticeably deeper deflation that would call for even more negative interest rates, thus prolonging the ELB episode. This result is not surprising since the rule-of-thumb firms set their prices based on past inflation and the inflation target, so in the absence of such firms, future real marginal costs have a larger impact on today's price set by the optimizing firms. In our second robustness exercise, we exclude the augmentation from the UIP condition; see equation (31). In our third exercise, we consider Cobb-Douglas technology in the second stage of production instead of the baseline Leontief production technology. We find that these two modifications marginally affect the impulse-response functions that we documented for our baseline model. In particular, ELB episodes have practically the same periodicity and duration as in our baseline model. In Appendix H, we describe these experiments in more details, and we illustrate the resulting responses with Fig. H.1.

[8] There is related recent literature on the transmission of liquidity trap from one country to another; see Bodenstein et al. (2016), Cook and Devereux (2016), and Corsetti et al. (2016) among others. See also Fernandez et al. (2017) for recent evidence on the importance of terms of trade shocks over the business cycle.

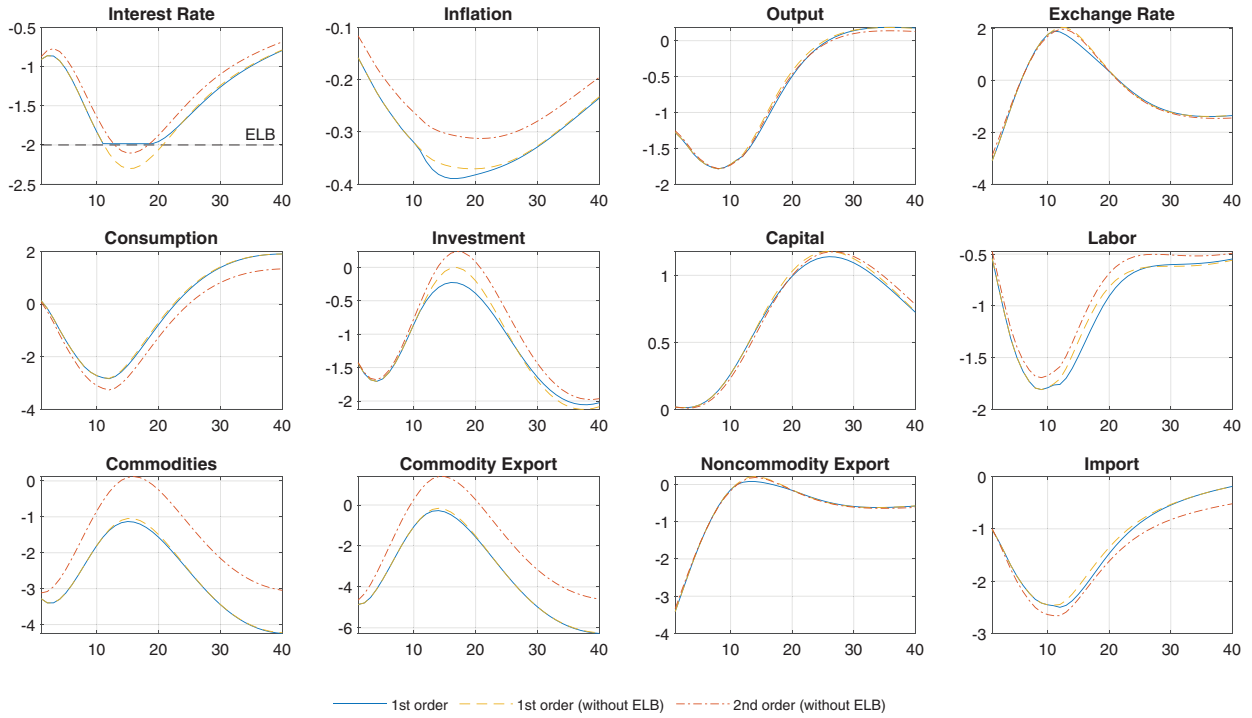

Fig. 5. Responses of linear and quadratic perturbation solutions in consumption demand scenario

4.2. Can we generate a realistic ELB episode using domestic shocks?

ELB episodes are difficult to generate in closed economies using domestic shocks.

As we have shown, it is fairly easy to generate realistic ELB episodes in our open-economy bToTEM model using foreign shocks. In contrast, the literature finds that ELB episodes are challenging to produce in closed-economy new Keynesian models using typical domestic shocks. In particular, Chung et al. (2012) find that standard structural models (e.g.; FRB/US; EDO; Smets and Wouters (2007)) deliver very low probability of hitting ELB. To generate the ELB episodes in a stylized new Keynesian model, Maliar and Maliar (2015) assume large 40-percent preference shocks affecting the marginal rate of substitution between consumption and leisure. Aruoba et al. (2018) augment the simulated series from the model to include historical data from the U.S. economy in order to obtain realistic spells at ELB. Fernández-Villaverde et al. (2015) argue that within the standard new Keynesian model, it is impossible to generate long ELB spells with modest drops in consumption, which were observed during the recent crises; they suggest that the only way to get around this result is to introduce wedges into the Euler equation. Also, Christiano et al. (2015) emphasize the importance of such shocks as a consumption wedge (a perturbation governing the accumulation of the risk-free asset), a financial wedge (a perturbation for optimal capital accumulation), a TFP shock, and a government consumption shock.

Realistic ELB episodes are also difficult to generate in open economies using only domestic shocks.

In our bToTEM simulation, the ELB episode is entirely due to foreign shocks. But would it be equally easy to generate a realistic ELB episode in the bToTEM model using domestic shocks? To answer this question, we build a domestic scenario in which the ELB episode is caused by a negative consumption demand shock.

The domestic shock acts during the first three years and then gradually declines. We calibrate the domestic demand shock to yield the same duration of the ELB episode as in the foreign demand scenario. The size of the shock at the peak is about 12 percent. The initial state of the economy is also the same as in the foreign-demand scenario.

The simulation of bToTEM under the consumption demand shock is shown in Fig. 5.

As we see, it is indeed possible to generate the ELB episode under the domestic demand shock but the model's implications are inconsistent with the stylized business cycle comovements. In particular, investment increases in response to negative demand shocks. Alternatives are not without flaws, for example, a negative supply shock is inflationary and counterfactually increases the interest rate according to the model's Taylor rule (see Fig. E.3). Thus, generating an appealing domestic ELB scenario is a challenge in the bToTEM model as well.

If our foreign demand and domestic demand scenarios appear extreme, we consider a mixed scenario in which the foreign and domestic shocks from the above two scenarios are taken with 0.5 weights. The results are shown in Fig. G.1 in Appendix G. The mixed scenario leads to a realistic ELB episode with responses that accord well with the business cycle comovements in the data, correcting thus the shortcomings of the pure domestic ELB scenario. On the basis of our experi-

ments, we conjecture that namely the presence of foreign shocks makes it possible to generate realistic ELB episodes rather than open-economy features of bToTEM.[9]

5. Understanding the role of nonlinearities in the bToTEM solution

In the past, policymakers were not concerned with nonlinearities in their large-scale macroeconomic models.[10] The question "How wrong could linearized solutions be?" became of interest to policymakers in light of the Great Recession and the ELB crisis. Since then, a considerable effort was dedicated to understanding the role of nonlinearities in the implications of new Keynesian models. In our baseline simulation of the Canadian ELB episode, the nonlinearity effects were modest but we found that variations in the model's parameterization and simulation scenarios make these effects quantitatively important. In this section, we show simulation experiments that highlight three effects of nonlinearity on the bToTEM solution:

i). ***(Uncertainty effect)****. Linearized solutions do not depend on the degree of volatility* σ*, as do nonlinear solutions.*
ii). ***(High-order effect)****. Linearization method neglects high-order polynomial terms, unlike more flexible nonlinear solutions.*
iii). ***(Solution-domain effect)****. Perturbation (local) solutions are constructed to be accurate in a deterministic steady state, and their accuracy can deteriorate dramatically when deviating from the steady state, in particular, in the area of ELB.*

Before discussing the simulation exercises, let us gain intuition into these three effects by looking at the perturbation solutions,

$$g(x,\sigma)\approx \underbrace{g(\bar{x},0)+g_x(\bar{x},0)(x-\bar{x})}_{\text{1st-order perturbation solution}}+\underbrace{\frac{1}{2}g_{\sigma\sigma}(\bar{x},0)\sigma^2}_{\text{uncertainty effect}}+\underbrace{\frac{1}{2}g_{xx}(\bar{x},0)(x-\bar{x})^2}_{\text{high-order effect}}, \tag{36}$$

where $g(x,\sigma)$ is a decision function to be approximated; x is a vector of state variables; σ is a degree of volatility; $(\bar{x},0)$ is a deterministic steady state; $g(\bar{x},0)$, $g_x(\bar{x},0)$ and $g_{xx}(\bar{x},0)$ are, respectively, steady state value, and Jacobian and Hessian matrices of g; $x-\bar{x}$ is a deviation from a steady state; $(x-\bar{x})^2\equiv(x-\bar{x})\otimes(x-\bar{x})$ is a tensor product of the deviations; the terms $g_\sigma(\bar{x},0)$ and $g_{\sigma x}(\bar{x},0)$ are omitted because they are shown to be equal to zero in rational expectations models; see Schmitt-Grohé and Uribe (2004).

As follows from (36), the second-order perturbation method addresses the effects i) and ii) by the *shift term* $\frac{1}{2}g_{\sigma\sigma}(\bar{x},0)\sigma^2$ and the *second-order term* $\frac{1}{2}g_{xx}(\bar{x},0)(x-\bar{x})^2$, respectively. However, plain perturbation methods do not address the effect iii) because they are constructed to be accurate in just one point – a deterministic steady state – and their quality can deteriorate when we deviate from the steady state, in particular, to the ELB area. Piecewise linear solutions produced by the IRIS and OccBin toolboxes help us correct the problem of the solution domain associated with ELB. However, the domain effect can be very large in new Keynesian models even in the absence of binding ELB.[11]

Our DL solution method addresses the effects i) - iii) more conclusively than the perturbation methods. First, it relies on a neural network approximation function which is more flexible than the first- and second-order polynomial functions; it can accurately account for the uncertainty and high-order effects. Second, it solves the model on a large ergodic-set domain which includes the ELB area instead of a small neighborhood of the steady-state point, so the accuracy of the DL solutions does not deteriorate as rapidly when deviating from the steady state as does the accuracy of local (perturbation) methods. We analyze the nonlinearity effects i), ii) and iii) on the bToTEM solution in Sections 5.1, 5.2 and 5.3, respectively.

5.1. The uncertainty effect and the inflation target

In this section, we illustrate the uncertainty effect in the context of a hypothetical increase in the inflation target from 2 to 3 percent. This experiment is of interest because in new Keynesian models, an increase in the inflation target reduces the probability of the ELB episodes. As an illustration, in Fig. 6 we show that if the Bank of Canada had the inflation target of 3 percent instead of 2 percent, ELB would never be reached in bToTEM under any solution method in our previous experiment.

The Bank of Canada revises its level of the inflation-control target every three to five years. The last revision was in 2016: the Bank of Canada considered the possibility of increasing the inflation target from 2 to 3 percent, but eventually it reached the decision to keep it at a 2-percent level for the next five years (because a higher inflation has certain costs for the Canadian economy; see Kryvtsov and Mendes (2015) for a discussion).

Dramatic differences between local and global solutions.

We implement the increase in the inflation target in bToTEM by maintaining the same real interest rate. We thus increase the nominal interest rate target level by one percent. The initial condition corresponds to the deterministic steady state of

[9] Our comparison of foreign and domestic shocks should be taken with caution because such shocks are not directly comparable. The foreign demand shock is closer in spirit to government shock in that it is exogenous demand for goods, not a shock that affects household or firm demand.

[10] As Bullard (2013) pointed out, "... the idea that U.S. policymakers should worry about the nonlinearity of the Taylor-type rule and its implications is sometimes viewed as an amusing bit of theory without real ramifications. Linear models tell you everything you need to know. And so, from the denial point of view, we can stick with our linear models..." Similarly, Leahy (2013) argues: "Prior to the crisis, it was easier to defend the proposition that nonlinearities were unimportant than it was to defend the proposition that nonlinearities were essential for understanding macroeconomic dynamics."

[11] Judd et al. (2017) demonstrate that approximation errors in linear and quadratic perturbation solutions to new Keynesian models can reach hundreds percent under empirically relevant calibrations, even if the economy is away from ELB.

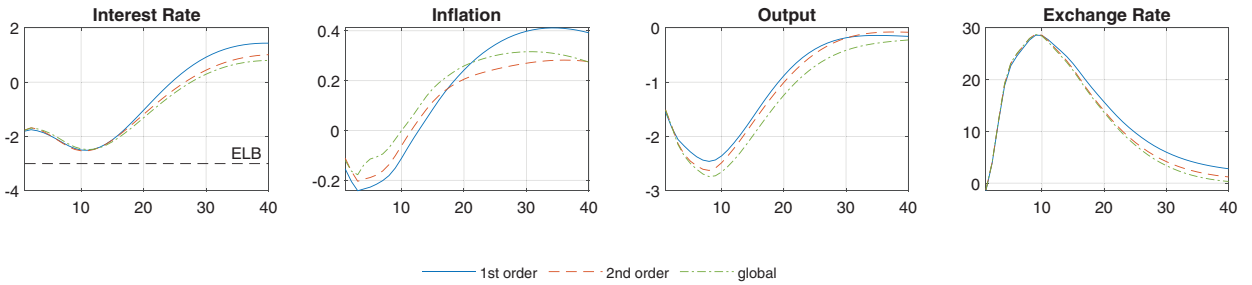

Fig. 6. Linear perturbation, quadratic perturbation, and global DL solutions under the inflation target of 3 percent (in deviations from the deterministic 3-percent inflation-target steady state)

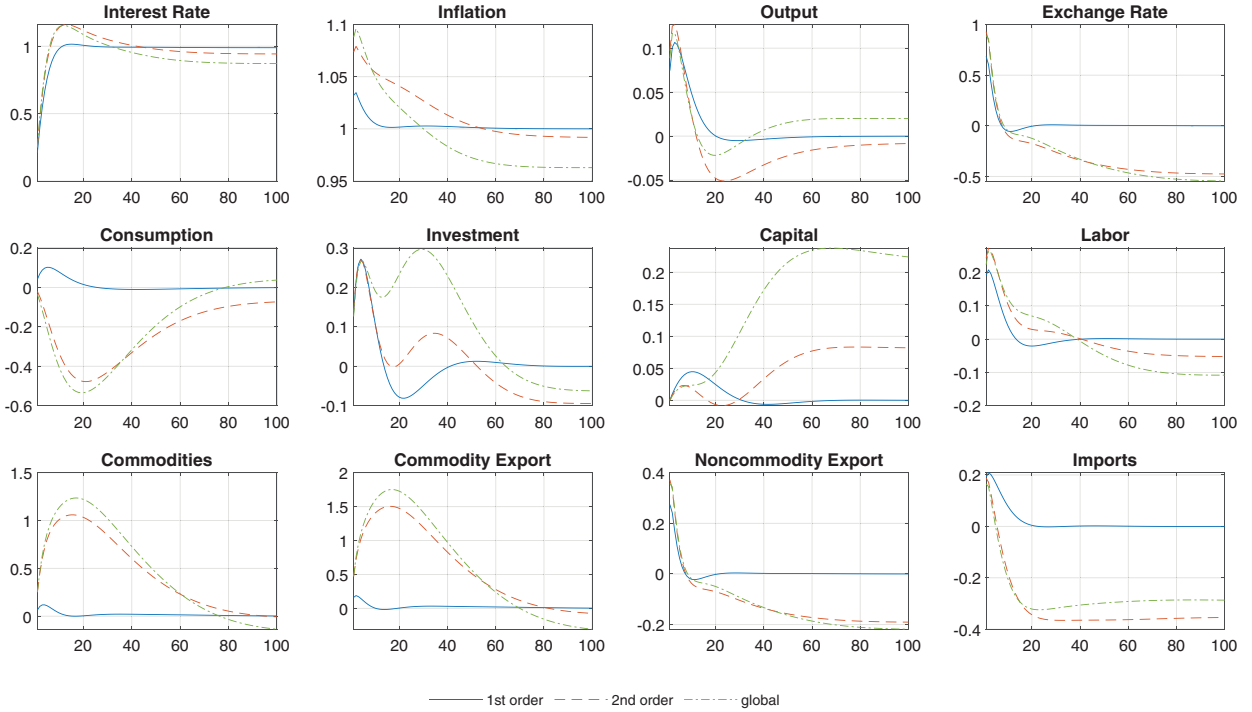

Fig. 7. A transition from a 2 percent to 3 percent inflation target under linear, quadratic, and global DL solutions (in deviations from the deterministic 2-percent inflation-target steady state)

the Canadian economy with an old inflation target of 2 percent. We recompute the solution under the new inflation target of 3 percent, and we simulate a transition path from that initial condition assuming no shocks over the transition path.

In Fig. 7, we show the transition path under the three solution methods. Evidently, the local and global solutions are dramatically different. The first-order perturbation solution behaves in a way that is typical for new Keynesian models, and it agrees with our intuition. The credible change in the inflation target almost instantaneously translates into an increase in the inflation rate. Inflation reacts so rapidly because in our sticky-price economy, the non-optimizing firms set their price according to the new inflation target. Following the Taylor rule with persistence, the interest rate remains below the new steady state during the transition and therefore provides a monetary stimulus. The stimulus is reflected in higher investment, output, consumption and capital. However, the second-order and global nonlinear solutions looks puzzling, in particular, consumption and investment produce wiggles and even go down. We will show that the puzzling behavior of nonlinear solutions is explained by the uncertainty effect.

Understanding the impact of uncertainty on the steady state.

Since ELB is not binding in this experiment, the first- and second-order perturbation solutions in (36) can differ either because of the uncertainty effect or because of the second-order effect. The uncertainty effect, represented by $\frac{1}{2}g^2_{\sigma\sigma}(\bar{x},0)\sigma^2$, implies that the linear and nonlinear models have different steady states, specifically, when the realized value of shocks is zero, a linear model converges to the deterministic steady state, while a nonlinear model converges to the so-called *risky steady state* that depends on a degree of volatility σ. The second-order effect, represented by $\frac{1}{2}g_{xx}(\bar{x},0)(x-\bar{x})^2$, includes nonlinearities associated with wage and price dispersions which are neglected by the linearization method. The uncertainty

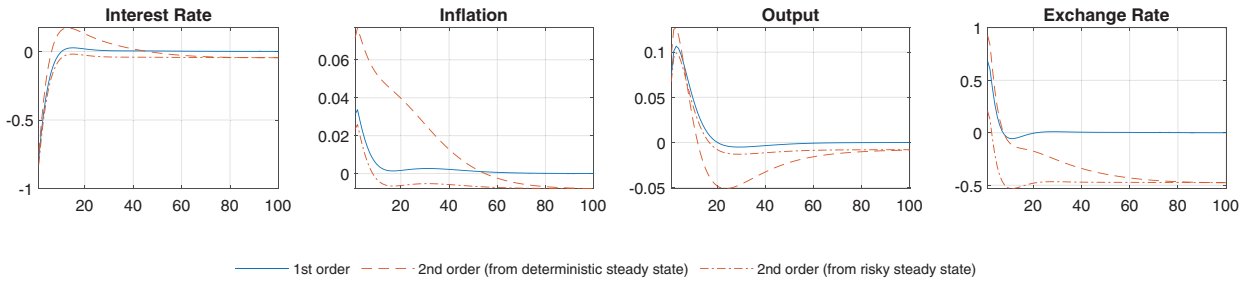

Fig. 8. A transition from a 2 percent to 3 percent inflation target under linear and two quadratic solutions one of which starts from the deterministic steady state and the other starts from the risky steady state (in deviations from the deterministic 3-percent inflation-target steady state)

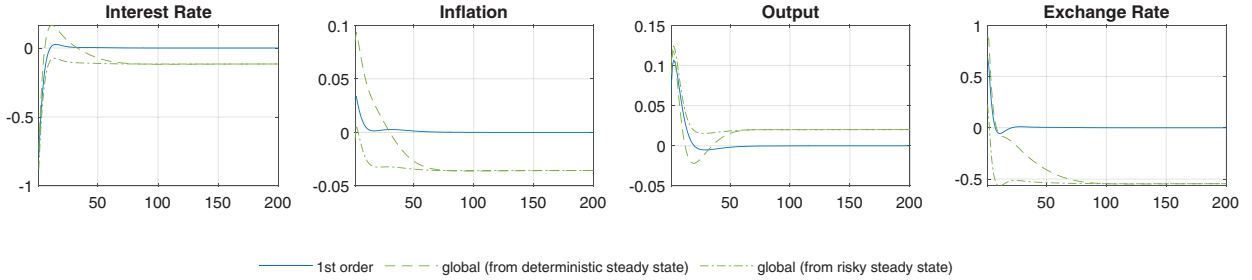

Fig. 9. A transition from a 2 percent to 3 percent inflation target under linear and two global DL solutions one of which starts from the deterministic steady state and the other starts from the risky steady state (in deviations from the deterministic 3-percent inflation-target steady state)

effect is well appreciated from Fig. 7. Both the second-order perturbation and global DL solutions converge not to the deterministic steady state but to some other levels.

To assess the relative importance of the uncertainty and second-order effects, in Fig. 8 we show a simulation of a second-order perturbation solution by using a risky steady state as an initial condition instead of the deterministic steady state. After the adjustment of the initial condition, the second-order effect disappears! Now, the first-order and alternative second-order perturbation solutions are visually indistinguishable, up to a constant term that shifts the second-order solution relative to the first-order solution. We thus recognize that the puzzling wiggly behavior of nonlinear solutions in Fig. 7 along the transition happens simply because nonlinear solutions are effectively confronted with two transitions: one is a transition to a new inflation target and the other is a transition from the deterministic to their own risky steady state. Adjusting the initial condition removes the second transition and makes the nonlinear solutions meaningful. Our results also mean that second-order effects associated with the wage and price dispersions plays only a minor role in the second-order perturbation solutions.

We next perform a similar experiment with the global DL solution by starting the transition from the risky steady state of the DL global solution; see Fig. 9. The results for the global DL solution are similar to those of the second-order perturbation solution. Here, we also observe an important uncertainty effects on the steady state but once we make an adjustment for differing steady states, the local and global solutions become qualitatively similar. However, nonlinearity plays a more important role in the global solution than in the perturbation solution, in particular, the long-term changes of the interest and inflation rates are visibly larger. The consequence of a larger stimulus is that the effect of the inflation-target change on output is positive for the global DL solution, while it was negative for the second-order perturbation solution.

The fact that linear and nonlinear solutions have different steady states is well known. A novel feature of our analysis is to show that the steady-state differences can lead to non-trivial differences in transition dynamics. We also offer a simple way to control for the steady-state effect, namely, we simulate each solution starting from its own steady state (alternatively, one can start at the same relative distance from the steady state). In our case, this eliminates the uncertainty effect and makes the simulated solutions to look like vertical translations of one another.

5.2. The high-order effect and the closing condition

In the previous section, the uncertainty effect was qualitatively important, while the high-order effect played a relatively minor role (provided that we make an adjustment for differing steady states). We now show an experiment in which the high-order effect is qualitatively important. We specifically revisit the simulation experiment in which the Canadian economy experiences three shocks to the ROW variables (Section 4.1). However, we modify the model's assumption by replacing the linear closing condition (35) that ensures stationarity in our baseline model with a similar closing condition in an ex-

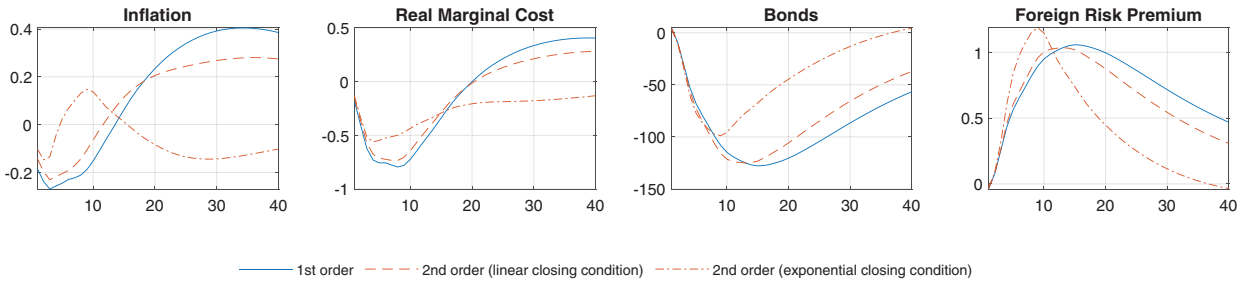

Fig. 10. Responses of linear perturbation, quadratic perturbation and alternative quadratic solutions to ROW shocks

ponential form, as is used in Schmitt-Grohé and Uribe (2003):

$$\kappa_t^f = \varsigma\left[\exp\left(\bar{b}^f - b_t^f\right) - 1\right]. \tag{37}$$

Recall that under the linear closing condition in Fig. 4, all three solutions looked very similar. However, the solutions in Fig. 10 look very different after we change the closing condition to (37). Now, the risk premium has a faster and sharper increase and decline because of the changes in the foreign bonds. The change in risk premium dynamics affects the exchange rate via the uncovered interest rate parity condition (31) (it pre-multiplies the foreign interest rate). In turn, the exchange rate affects the prices of two out of four inputs in the production function, which eventually impacts the real marginal cost and inflation.

Why are the nonlinearities of the closing condition manifested in bToTEM? The linear closing condition (35) does not have second-order terms by construction and its linearization is equal to the condition itself $\kappa_t^f = \varsigma\left(\bar{b}^f - b_t^f\right)$. In contrast, the exponential closing condition (37) does have high-order terms, specifically, $\kappa_t^f \approx \varsigma\left(\bar{b}^f - b_t^f\right) + \frac{1}{2}\varsigma\left(\bar{b}^f - b_t^f\right)^2$. Such high-order terms account for a visibly large difference between the linear and nonlinear perturbation solutions in Fig. 10.

The importance of stationarity condition in the bToTEM model is surprising, given a well-known result of Schmitt-Grohé and Uribe (2003) that a specific closing condition used does not significantly affect the implications of open-economy models. However, we shall recall that their analysis focuses exclusively on linearized solutions. Under linearization, the exponential closing condition (37) is given by $\kappa_t^f \approx \varsigma\left(\bar{b}^f - b_t^f\right)$, i.e., it coincides exactly with the linear closing condition (35). Thus, the analysis of Schmitt-Grohé and Uribe (2003) would treat the two alternative closing conditions as identical and would not reveal the importance of high-order effects associated with the closing condition as our nonlinear analysis does.

Our analysis does not provide a theoretical stand on what a particular specification of the closing condition to choose. However, we find an important practical consideration: the closing condition in exponential form used in Schmitt-Grohé and Uribe (2003) tend to produce explosive simulation, while our linear closing condition leads to numerically-stable simulation. Again, the difference between these two closing conditions only matters for simulation of nonlinear solutions.

5.3. The solution-domain effect and the ELB irrelevance

In Fig. 4, bToTEM simulation predicts nearly the same magnitude and duration of the ELB episode with and without the ELB constraint. The inclusion of such constraint does not significantly affect the variables other than interest rate. Furthermore, local (perturbation) and global solutions look very similar. Taken together, these results imply that the domain effect iii) is modest. That it, the global DL solution constructed to be accurate on a large domain including the ELB area turned out to be similar to the perturbation solutions constructed in a single steady-state point by neglecting ELB. In that specific experiment, the Bank of Canada would not be terribly wrong if it just used a plain first-order perturbation method for analyzing their ToTEM model, either ignoring ELB entirely or chopping off the interest rate at the ELB level in simulation. In the remainder of this section, we explore reasons for the ELB irrelevance in our analysis.

The findings of the literature on the importance of ELB are mixed.

Let us recall the findings of the related literature. Several papers find that ELB is quantitatively important in the context of stylized new Keynesian models with Calvo pricing. In particular, Maliar and Maliar (2015) argue that first- and second-order perturbation solutions understate the severity and duration of the ELB crisis. Fernández-Villaverde et al. (2015) show that in the periods of binding ELB, the nonlinearities start playing an important role, affecting the expected duration of spells, fiscal multipliers, as well as the trade-off between spells and drops in consumption. Aruoba et al. (2018) show that nonlinearities in their new Keynesian model can explain the differential experience of the U.S. and Japan by allowing for nonfundamental shocks (sunspots). Furthermore, in the model with Rotemberg pricing, Boneva et al. (2016) find that linearization considerably distorts interactions between ELB and the agents' decision rules, in particular, those for labor supply; see also Gust et al. (2012) for related evidence from estimation of a nonlinear new Keynesian model.

However, there is also literature that finds that the ELB constraint is quantitatively unimportant. In particular, Christiano et al. (2016) study a stable-under-learning rational expectation equilibrium in a simple nonlinear model with Calvo pricing;

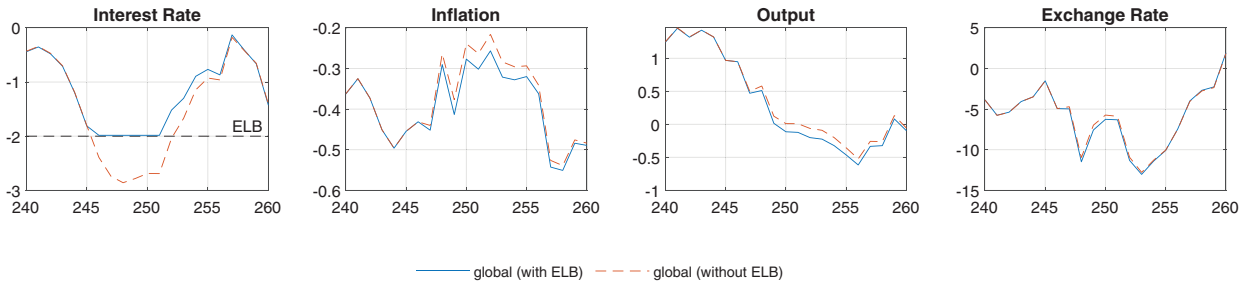

Fig. 11. Simulated series

they find that a linearized model inherits the key properties of the nonlinear model for fiscal policy at ELB, predicting similar government spending multipliers and output drops. Furthermore, Eggertsson and Singh (2016) derive a closed-form nonlinear solution to a simple, two-equation new Keynesian model; they report negligible differences between the exact and linearized solutions when they look at the effects of fiscal policy at ELB.

Irrelevance of ELB without room for unconventional policy.

A recent paper of Debortoli et al. (2019) coined the term *irrelevance of the ELB hypothesis* to refer to the case when the impact of ELB on the economy is insignificant. However, the irrelevance in Debortoli et al. (2019) has a different meaning than the one in our analysis. They argue that ELB was not a relevant constraint since monetary policymakers engaged in unconventional monetary policies (forward guidance, quantitative easing, balance-sheet policies, negative interest rates) to overcome the limitations posed by ELB. In contrast to Debortoli et al. (2019), we obtain the ELB irrelevance result without room for unconventional monetary policy. Our irrelevance result does not mean that the Great Recession was unimportant in Canada but suggests that the recession dynamics was not overwhelmingly amplified by a binding the ELB constraint.[12]

A minor role of ELB in the bToTEM risky steady state.

Our baseline economy with 2 percent inflation target matches well the ELB statistics of Canadian economy as captured by ToTEM (see Dorich et al. (2018). To be specific, the probability of reaching ELB in bToTEM is about 8 percent and the average duration of ELB episodes is 5 quarters. Such a significant probability of reaching ELB affects the average interest rate, but we find that the effect of ELB on the first moments of the other key model variables is very small. A typical stochastic simulation with and without ELB is shown in Fig. 11.

We find that the difference between the unconditional means of the interest rate in the models with and without ELB is 5.5 basis points, while the corresponding difference in inflation is only 0.4 basis points. Such difference is also documented by Hills et al. (2016) in the context of their estimation of deflationary bias in the U.S. economy. It means that in a nonlinear model, the central bank does not get the same inflation rate as it targets by the Taylor rule. However, Hills et al. (2016) report far more substantial deflationary bias due to ELB than we do, specifically, they find the difference between the risky steady states of inflation in the models with and without ELB to be 18 basis points.

Why is there so large difference between the estimates of Hills et al. (2016) and those in the present paper? Hills et al. (2016) argue that a critical ingredient for their result is the assumption of the optimizing price setters that are forward looking and that take into account a tail risk in the future marginal costs. In contrast, the presence of rule-of-thumb price setters in bToTEM diminishes the contribution of future marginal costs to the pricing decision (the rule-of-thumb agents were introduced in ToTEM to address the forward guidance puzzle). This is precisely the feature that accounts for the minor role of ELB in the quantitative implications of the bToTEM model.

6. Conclusion

This paper tells a tale of the Canadian the ELB experience during the Great Recession. We demonstrate that a direct impact on the foreign trade was a quantitatively important transmission channel through which the contagion of the Great Recession spread to Canada from the rest of the world. There is a popular saying “When the U.S. sneezes, Canada catches a cold”. But this time it went the other way around: it was the U.S. that caught the (subprime crisis) cold, and it was Canada that sneezed.

Our tale builds around a carefully designed bToTEM model, which is meticulously calibrated to reproduce the key observations on the Canadian economy, as well as the impulse responses of ToTEM. The bToTEM model is capable of generating a realistic ELB episode under the rest-of-the-world shocks calibrated from the full-scale ToTEM model.

Large-scale central banking models like ToTEM and bToTEM are routinely used for policy experiments but their analysis is limited to linear approximations. Our novel DL algorithm combines supervised and unsupervised learning in a way

[12] Debortoli et al. (2019) mention that their irrelevance result could be captured by specifying the Taylor rule to smooth on a notional interest rate, rather than on the observed interest rate, and then imposing ZLB. We ran additional experiments and we found that the introduction of the notional interest rate indeed makes ELB even less important in our analysis (these results are not reported).

that enables us to construct an accurate global fully nonlinear solution to a central banking model with the degrees of nonlinearities and the size of the state space that have not been studied before.

What is the value added of deep learning for telling the Canadian ELB tale? It is fair to say that we could have discovered and simulated the ELB contagion mechanism by using exclusively linearization-based methods. But we would not know how reliable our linear solution is, and we would miss some dramatic effects of nonlinearities on the predictions of the bToTEM model. In particular, we would overlook the uncertainty effect that makes the steady states of linear and nonlinear models to differ and that accounts for observed qualitative differences in the transitional dynamics of the two models. Furthermore, we would miss the nonlinearity effects associated with the closing condition. On the other hand, the nonlinearity associated with ELB turned out to be of a lesser importance than we expected.

The bToTEM model constructed in the paper is a useful alternative model to the Bank of Canada. While the full-scale ToTEM is not yet feasible for global nonlinear methods, bToTEM can be solved nonlinearly and its accuracy can be assessed. In addition to the Bank of Canada, our deep learning analysis can be useful to all users of large-scale models, including researchers, central banks and government agencies who can benefit from our methodology of calibrating, solving, and simulating large-scale macroeconomic models, as well as designing nontrivial policy experiments within such models.

Appendix A. Derivation of the optimality conditions

In this appendix, we elaborate the derivation of the optimality conditions.

A1. Production of final goods

First stage of production

The Lagrangian of the problem is

$$E_0\sum_{t=0}^{\infty}\mathcal{R}_{0,t}\Bigg(P_t^z\Bigg(\Big(\delta_l(A_tL_t)^{\frac{\sigma-1}{\sigma}}+\delta_k(u_tK_t)^{\frac{\sigma-1}{\sigma}}+\delta_{com}\big(COM_t^d\big)^{\frac{\sigma-1}{\sigma}}+\delta_m(M_t)^{\frac{\sigma-1}{\sigma}}\Big)^{\frac{\sigma}{\sigma-1}}$$
$$-\frac{\chi_i}{2}\Big(\frac{I_t}{I_{t-1}}-1\Big)^2I_t\Bigg)-W_tL_t-P_t^{com}COM_t^d-P_t^iI_t-P_t^mM_t+Q_t\left((1-d_t)K_t+I_t-K_{t+1}\right)\Bigg).$$

The optimal quantities satisfy the following conditions, with an augmented discount factor as in ToTEM:

$$W_t=P_t^z\big(Z_t^g\big)^{\frac{1}{\sigma}}\delta_l(A_t)^{\frac{\sigma-1}{\sigma}}(L_t)^{\frac{-1}{\sigma}} \tag{A.1}$$

$$Q_t=\frac{1}{R_t^k}E_t\Big[P_{t+1}^z\big(Z_{t+1}^g\big)^{\frac{1}{\sigma}}\delta_k(u_{t+1})^{\frac{\sigma-1}{\sigma}}(K_{t+1})^{\frac{-1}{\sigma}}+Q_{t+1}(1-d_{t+1})\Big] \tag{A.2}$$

$$P_t^i=Q_t-P_t^z\frac{\chi_i}{2}\Big(\frac{I_t}{I_{t-1}}-1\Big)\Big(\frac{3I_t}{I_{t-1}}-1\Big)+\frac{1}{R_t^k}E_t\Big[P_{t+1}^z\chi_i\Big(\frac{I_{t+1}}{I_t}-1\Big)\Big(\frac{I_{t+1}}{I_t}\Big)^2\Big] \tag{A.3}$$

$$P_t^{com}=P_t^z\big(Z_t^g\big)^{\frac{1}{\sigma}}\delta_{com}\big(COM_t^d\big)^{\frac{-1}{\sigma}} \tag{A.4}$$

$$P_t^m=P_t^z\big(Z_t^g\big)^{\frac{1}{\sigma}}\delta_m(M_t)^{\frac{-1}{\sigma}} \tag{A.5}$$

$$Q_t\bar{d}\rho e^{\rho(u_t-1)}=P_t^z\big(Z_t^g\big)^{\frac{1}{\sigma}}\delta_k(u_t)^{\frac{-1}{\sigma}}(K_t)^{\frac{-1}{\sigma}} \tag{A.6}$$

where Q_t is the Lagrange multiplier on the law of motion of capital (3). Introducing real prices by $p_t^z=P_t^z/P_t$, $w_t=W_t/P_t$, $p_t^i=P_t^i/P_t$, $p_t^{com}=P_t^{com}/P_t$, $p_t^m=P_t^m/P_t$, and $q_t=Q_t/P_t$, where P_t is the price of final good, the conditions can be written as

$$w_t=p_t^z\big(Z_t^g\big)^{\frac{1}{\sigma}}\delta_l(A_t)^{\frac{\sigma-1}{\sigma}}(L_t)^{\frac{-1}{\sigma}} \tag{A.7}$$

$$q_t=\frac{1}{R_t^k}E_t\Big[\pi_{t+1}\Big(p_{t+1}^z\big(Z_{t+1}^g\big)^{\frac{1}{\sigma}}\delta_k(u_{t+1})^{\frac{\sigma-1}{\sigma}}(K_{t+1})^{\frac{-1}{\sigma}}+q_{t+1}(1-d_{t+1})\Big)\Big] \tag{A.8}$$

$$p_t^i=q_t-p_t^z\frac{\chi_i}{2}\Big(\frac{I_t}{I_{t-1}}-1\Big)\Big(\frac{3I_t}{I_{t-1}}-1\Big)+\frac{1}{R_t^k}E_t\Big[\pi_{t+1}p_{t+1}^z\chi_i\Big(\frac{I_{t+1}}{I_t}-1\Big)\Big(\frac{I_{t+1}}{I_t}\Big)^2\Big] \tag{A.9}$$

$$p_t^{com}=p_t^z\big(Z_t^g\big)^{\frac{1}{\sigma}}\delta_{com}\big(COM_t^d\big)^{\frac{-1}{\sigma}} \tag{A.10}$$

$$p_t^m = p_t^z \left(Z_t^g\right)^{\frac{1}{\sigma}} \delta_m (M_t)^{\frac{-1}{\sigma}} \tag{A.11}$$

$$q_t \bar{d} \rho e^{\rho(u_t-1)} = p_t^z \left(Z_t^g\right)^{\frac{1}{\sigma}} \delta_k (u_t)^{\frac{-1}{\sigma}} (K_t)^{\frac{-1}{\sigma}} \tag{A.12}$$

Second stage of production

The first-order condition associated with the problem (9)-(10) is

$$E_t\left[\sum_{j=0}^{\infty} \theta^j \mathcal{R}_{t,t+j} Z_{i,t+j} \left(\prod_{k=1}^{j} \bar{\pi}_{t+k}(1-\varepsilon) + \varepsilon \frac{(1-s_m)P_{t+j}^z + s_m P_{t+j}}{P_t^*}\right)\right] = 0,$$

or using the demand function (10)

$$E_t\left[\sum_{j=0}^{\infty} (\beta\theta)^j \lambda_{t+j} \left(\frac{\prod_{k=1}^{j} \bar{\pi}_{t+k}}{\prod_{k=1}^{j} \pi_{t+k}}\right)^{-\varepsilon} Z_{t+j} \left(\frac{\prod_{k=1}^{j} \bar{\pi}_{t+k}}{\prod_{k=1}^{j} \pi_{t+k}} \frac{P_t^*}{P_t} - \frac{\varepsilon}{\varepsilon-1} rmc_{t+j}\right)\right] = 0, \tag{A.13}$$

where the real marginal cost is

$$rmc_t = (1-s_m)\frac{P_t^z}{P_t} + s_m. \tag{A.14}$$

The condition (A.13) can be written as

$$\frac{P_t^*}{P_t} = \frac{F_{1t}}{F_{2t}} \tag{A.15}$$

$$F_{1t} \equiv E_t\left[\sum_{j=0}^{\infty} (\beta\theta)^j \lambda_{t+j} \left(\frac{\prod_{k=1}^{j} \bar{\pi}_{t+k}}{\prod_{k=1}^{j} \pi_{t+k}}\right)^{-\varepsilon} Z_{t+j} \frac{\varepsilon}{\varepsilon-1} rmc_{t+j}\right]$$

$$F_{2t} \equiv E_t\left[\sum_{j=0}^{\infty} (\beta\theta)^j \lambda_{t+j} \left(\frac{\prod_{k=1}^{j} \bar{\pi}_{t+k}}{\prod_{k=1}^{j} \pi_{t+k}}\right)^{1-\varepsilon} Z_{t+j}\right].$$

The equations for F_{1t} and F_{2t} can be written recursively as

$$F_{1t} = \lambda_t Z_t \frac{\varepsilon}{\varepsilon-1} rmc_t + \beta\theta E_t\left[\left(\frac{\bar{\pi}_{t+1}}{\pi_{t+1}}\right)^{-\varepsilon} F_{1t+1}\right], \tag{A.16}$$

$$F_{2t} = \lambda_t Z_t + \beta\theta E_t\left[\left(\frac{\bar{\pi}_{t+1}}{\pi_{t+1}}\right)^{1-\varepsilon} F_{2t+1}\right]. \tag{A.17}$$

The aggregate price introduced by (7) satisfies the following condition:

$$\theta\left(\frac{\bar{\pi}_t}{\pi_t}\right)^{1-\varepsilon} + (1-\theta)\omega\left(\frac{(\pi_{t-1})^{\gamma}(\bar{\pi}_t)^{1-\gamma}}{\pi_t}\right)^{1-\varepsilon} + (1-\theta)(1-\omega)\left(\frac{P_t^*}{P_t}\right)^{1-\varepsilon} = 1. \tag{A.18}$$

Combining (A.18) with the optimal price setting (A.15), we get

$$\theta\left(\frac{\bar{\pi}_t}{\pi_t}\right)^{1-\varepsilon} + (1-\theta)\omega\left(\frac{(\pi_{t-1})^{\gamma}(\bar{\pi}_t)^{1-\gamma}}{\pi_t}\right)^{1-\varepsilon} + (1-\theta)(1-\omega)\left(\frac{F_{1t}}{F_{2t}}\right)^{1-\varepsilon} = 1. \tag{A.19}$$

Relation between the first and second stages of production

Introducing the following price index

$$\bar{P}_t = \left(\int_0^1 P_{it}^{-\varepsilon} di\right)^{\frac{-1}{\varepsilon}},$$

which can be expressed using the price settings of the rule-of-thumb and forward-looking firms as follows:

$$\left(\frac{\bar{P}_t}{P_t}\right)^{-\varepsilon} = \theta\left(\frac{\bar{\pi}\bar{P}_{t-1}}{P_t}\right)^{-\varepsilon} + (1-\theta)\omega\left(\frac{(\pi_{t-1})^{\gamma}(\bar{\pi}_t)^{1-\gamma}\bar{P}_{t-1}}{P_t}\right)^{-\varepsilon} + (1-\theta)(1-\omega)\left(\frac{P_t^*}{P_t}\right)^{-\varepsilon},$$

the dynamics of the price dispersion is the following:

$$\Delta_t = \theta\left(\frac{\bar{\pi}_t}{\pi_t}\right)^{-\varepsilon}\Delta_{t-1} + (1-\theta)\omega\left(\frac{(\pi_{t-1})^{\gamma}(\bar{\pi}_t)^{1-\gamma}}{\pi_t}\right)^{-\varepsilon}\Delta_{t-1} + (1-\theta)(1-\omega)\left(\frac{F_{1t}}{F_{2t}}\right)^{-\varepsilon}. \tag{A.20}$$

A2. Commodities

The Lagrangian of the problem is the following:

$$E_0\sum_{t=0}^{\infty}\mathcal{R}_{0,t}\left(P_t^{com}\left((Z_t^{com})^{s_z}(A_tL)^{1-s_z}-\frac{\chi_{com}}{2}\left(\frac{Z_t^{com}}{Z_{t-1}^{com}}-1\right)^2Z_t^{com}\right)-P_tZ_t^{com}\right).$$

The resulting partial adjustment equation for the commodity-producing firm is as follows:

$$P_t=P_t^{com}\frac{s_zCOM_t}{Z_t^{com}}-P_t^{com}\frac{\chi_{com}}{2}\left(\frac{Z_t^{com}}{Z_{t-1}^{com}}-1\right)\left(\frac{3Z_t^{com}}{Z_{t-1}^{com}}-1\right)+\frac{1}{R_t}E_t\left[P_{t+1}^{com}\chi_{com}\left(\frac{Z_{t+1}^{com}}{Z_t^{com}}-1\right)\left(\frac{Z_{t+1}^{com}}{Z_t^{com}}\right)^2\right],\tag{A.21}$$

or expressed in real prices

$$1=p_t^{com}\frac{s_zCOM_t}{Z_t^{com}}-p_t^{com}\frac{\chi_{com}}{2}\left(\frac{Z_t^{com}}{Z_{t-1}^{com}}-1\right)\left(\frac{3Z_t^{com}}{Z_{t-1}^{com}}-1\right)+\frac{1}{R_t}E_t\left[\pi_{t+1}p_{t+1}^{com}\chi_{com}\left(\frac{Z_{t+1}^{com}}{Z_t^{com}}-1\right)\left(\frac{Z_{t+1}^{com}}{Z_t^{com}}\right)^2\right].\tag{A.22}$$

A3. Imports

Similarly to (A.13), the first-order optimality condition associated with the problem of optimizing forward-looking importers is the following:

$$E_t\left[\sum_{j=0}^{\infty}(\beta\theta_m)^j\lambda_{t+j}M_{i,t+j}\left(\frac{\prod_{k=1}^{j}\bar{\pi}_{t+k}}{\prod_{k=1}^{j}\pi_{t+k}}\frac{P_t^{m*}}{P_t}-\frac{\varepsilon_m}{\varepsilon_m-1}\frac{e_{t+j}P_{t+j}^{mf}}{P_{t+j}}\right)\right]=0.\tag{A.23}$$

The condition (A.23) can be written as

$$\frac{P_t^{m*}}{P_t}=\frac{F_{1t}^m}{F_{2t}^m},\tag{A.24}$$

where F_{1t}^m and F_{2t}^m are given by the following equations:

$$F_{1t}^m=\lambda_tM_t\frac{\varepsilon_m}{\varepsilon_m-1}s_tp_t^{mf}+\beta\theta_mE_t\left[\left(\frac{\bar{\pi}_{t+1}}{\pi_{t+1}^m}\right)^{-\varepsilon_m}F_{1t+1}^m\right],\tag{A.25}$$

$$F_{2t}^m=\lambda_tM_t+\beta\theta_mE_t\left[\frac{\bar{\pi}_{t+1}}{\pi_{t+1}}\left(\frac{\bar{\pi}_{t+1}}{\pi_{t+1}^m}\right)^{-\varepsilon_m}F_{2t+1}^m\right],\tag{A.26}$$

and where s_t and p_t^{mf} are the real exchange rate and the real foreign price of imports introduced by $s_t=e_tP_t^f/P_t$ and $p_t^{mf}=P_t^{mf}/P_t^f$, respectively. The aggregate import price satisfies the following condition:

$$\theta_m\left(\frac{\bar{\pi}_t}{\pi_t^m}\right)^{1-\varepsilon_m}+(1-\theta_m)\omega_m\left(\frac{(\pi_{t-1}^m)^{\gamma_m}(\bar{\pi}_t)^{1-\gamma_m}}{\pi_t^m}\right)^{1-\varepsilon_m}+(1-\theta_m)(1-\omega_m)\left(\frac{P_t^{m*}}{P_t^m}\right)^{1-\varepsilon_m}=1.\tag{A.27}$$

Combining (A.27) with (A.24), we get

$$\theta_m\left(\frac{\bar{\pi}_t}{\pi_t^m}\right)^{1-\varepsilon_m}+(1-\theta_m)\omega_m\left(\frac{(\pi_{t-1}^m)^{\gamma_m}(\bar{\pi}_t)^{1-\gamma_m}}{\pi_t^m}\right)^{1-\varepsilon_m}+(1-\theta_m)(1-\omega_m)\left(\frac{F_{1t}^m}{p_t^mF_{2t}^m}\right)^{1-\varepsilon_m}=1.\tag{A.28}$$

A4. Households

The maximization of the lifetime utility (16) subject to the budget constraint (17) with respect to consumption and bond holdings yields the following first-order condition:

$$E_t\left[\beta\frac{\lambda_{t+1}}{\lambda_t}\frac{R_tP_t}{P_{t+1}}\right]=1,\tag{A.29}$$

where λ_t is the marginal utility of consumption, which is given by

$$\lambda_t=(C_t-\xi C_{t-1})^{\frac{-1}{\mu}}\exp\left(\frac{\eta(1-\mu)}{\mu(1+\eta)}\int_0^1(L_{ht})^{\frac{\eta+1}{\eta}}dh\right)\eta_t^c.\tag{A.30}$$

The no-arbitrage condition on holdings of domestic and foreign bonds would imply the following interest rate parity:

$$e_t = E_t\left[\frac{e_{t+1}R_t^f\left(1+\kappa_t^f\right)}{R_t}\right],$$

which is further augmented as in ToTEM to improve business cycle properties of the model as follows:

$$e_t = E_t\left[(e_{t-1})^{\varkappa}\left(e_{t+1}\frac{R_t^f\left(1+\kappa_t^f\right)}{R_t}\right)^{1-\varkappa}\right]. \tag{A.31}$$

The condition can be expressed in terms of real exchange rate $s_t = e_t P_t^f/P_t$ as follows:

$$s_t = E_t\left[\left(s_{t-1}\frac{\pi_t^f}{\pi_t}\right)^{\varkappa}\left(s_{t+1}\frac{R_t^f\left(1+\kappa_t^f\right)}{R_t}\frac{\pi_{t+1}}{\pi_{t+1}^f}\right)^{1-\varkappa}\right]. \tag{A.32}$$

A5. Wage setting

The first-order optimality condition associated with the problem (21)-(22) is

$$E_t\left[\sum_{j=0}^{\infty}(\beta\theta_w)^j\left(U_{C,t+j}\frac{\prod_{k=1}^{j}\bar{\pi}_{t+k}}{P_{t+j}}\left(L_{h,t+j}+W_t^*\frac{\partial L_{h,t+j}}{\partial W_t^*}\right)+U_{Lh,t+j}\frac{\partial L_{h,t+j}}{\partial W_t^*}\right)\right]=0,$$

where

$$U_{Ct} = (C_t-\xi C_{t-1})^{\frac{-1}{\mu}}\exp\left(\frac{\eta(1-\mu)}{\mu(1+\eta)}\int_0^1 (L_{ht})^{\frac{\eta+1}{\eta}}dh\right)\eta_t^c$$

$$U_{Lh,t} = -(C_t-\xi C_{t-1})^{\frac{\mu-1}{\mu}}\exp\left(\frac{\eta(1-\mu)}{\mu(1+\eta)}\int_0^1 (L_{ht})^{\frac{\eta+1}{\eta}}dh\right)(L_{ht})^{\frac{1}{\eta}}\eta_t^c$$

$$\frac{\partial L_{h,t+j}}{\partial W_t^*} = \frac{-\varepsilon_w}{W_t^*}L_{h,t+j}$$

or

$$E_t\left[\sum_{j=0}^{\infty}(\beta\theta_w)^j U_{C,t+j}L_{h,t+j}\left(\frac{\prod_{k=1}^{j}\bar{\pi}_{t+k}}{\prod_{k=1}^{j}\pi_{t+k}}\frac{W_t^*}{P_t}-\frac{\varepsilon_w}{\varepsilon_w-1}MRS_{h,t+j}\right)\right]=0, \tag{A.33}$$

where the marginal rate of substitution between consumption and labor is introduced as follows:

$$MRS_{h,t} \equiv \frac{-U_{Lh,t}}{U_{C,t}} = (C_t-\xi C_{t-1})(L_{ht})^{\frac{1}{\eta}}.$$

Using the demand (22), we write the optimality condition (A.33) as

$$E_t\left[\sum_{j=0}^{\infty}(\beta\theta_w)^j\lambda_{t+j}\left(\frac{\prod_{k=1}^{j}\bar{\pi}_{t+k}}{\prod_{k=1}^{j}\pi_{t+k}}\left(\frac{\prod_{k=1}^{j}\bar{\pi}_{t+k}W_t^*}{\prod_{k=1}^{j}\pi_{t+k}^w W_t}\right)^{-\varepsilon_w}L_{t+j}\frac{W_t^*}{P_t}\right.\right.$$
$$\left.\left.-\frac{\varepsilon_w}{\varepsilon_w-1}\left(C_{t+j}-\xi C_{t+j-1}\right)\left(\frac{\prod_{k=1}^{j}\bar{\pi}_{t+k}W_t^*}{\prod_{k=1}^{j}\pi_{t+k}^w W_t}\right)^{\frac{-\varepsilon_w(1+\eta)}{\eta}}\left(L_{t+j}\right)^{\frac{1+\eta}{\eta}}\right)\right]=0, \tag{A.34}$$

or

$$E_t\left[\sum_{j=0}^{\infty}(\beta\theta_w)^j\lambda_{t+j}\left(\frac{\prod_{k=1}^{j}\bar{\pi}_{t+k}}{\prod_{k=1}^{j}\pi_{t+k}}\left(\frac{\prod_{k=1}^{j}\bar{\pi}_{t+k}}{\prod_{k=1}^{j}\pi_{t+k}^w}\right)^{-\varepsilon_w}L_{t+j}\left(\frac{W_t^*}{W_t}\right)^{\frac{\varepsilon_w}{\eta}}\frac{W_t^*}{P_t}\right.\right.$$
$$\left.\left.-\frac{\varepsilon_w}{\varepsilon_w-1}\left(\frac{\prod_{k=1}^{j}\bar{\pi}_{t+k}}{\prod_{k=1}^{j}\pi_{t+k}^w}\right)^{\frac{-\varepsilon_w(1+\eta)}{\eta}}\left(C_{t+j}-\xi C_{t+j-1}\right)\left(L_{t+j}\right)^{\frac{1+\eta}{\eta}}\right)\right]=0. \tag{A.35}$$

Introducing $w_t^* = W_t^*/P_t$, the condition (A.34) can be stated as

$$(w_t^*)^{1+\frac{\varepsilon_w}{\eta}}(w_t)^{\frac{-\varepsilon_w}{\eta}} = \frac{F_{1t}^w}{F_{2t}^w} \tag{A.36}$$

$$F_{1t}^{w} \equiv E_t\left[\sum_{j=0}^{\infty}(\beta\theta_w)^j\lambda_{t+j}\frac{\varepsilon_w}{\varepsilon_w-1}\left(\frac{\prod_{k=1}^{j}\bar{\pi}_{t+k}}{\prod_{k=1}^{j}\pi_{t+k}^{w}}\right)^{\frac{-\varepsilon_w(1+\eta)}{\eta}}\left(C_{t+j}-\xi C_{t+j-1}\right)\left(L_{t+j}\right)^{\frac{1+\eta}{\eta}}\right]$$

$$F_{2t}^{w} \equiv E_t\left[\sum_{j=0}^{\infty}(\beta\theta_w)^j\lambda_{t+j}\frac{\prod_{k=1}^{j}\bar{\pi}_{t+k}}{\prod_{k=1}^{j}\pi_{t+k}}\left(\frac{\prod_{k=1}^{j}\bar{\pi}_{t+k}}{\prod_{k=1}^{j}\pi_{t+k}^{w}}\right)^{-\varepsilon_w}L_{t+j}\right]$$

The equations for F_{1t}^{w} and F_{2t}^{w} can be written recursively as

$$F_{1t}^{w} = \lambda_t\frac{\varepsilon_w}{\varepsilon_w-1}(C_t-\xi C_{t-1})(L_t)^{\frac{1+\eta}{\eta}} + \beta\theta_w E_t\left[\left(\frac{\bar{\pi}_{t+1}}{\pi_{t+1}^{w}}\right)^{\frac{-\varepsilon_w(1+\eta)}{\eta}}F_{1,t+1}^{w}\right] \tag{A.37}$$

and

$$F_{2t}^{w} = \lambda_t L_t + \beta\theta_w E_t\left[\frac{\bar{\pi}_{t+1}}{\pi_{t+1}}\left(\frac{\bar{\pi}_{t+1}}{\pi_{t+1}^{w}}\right)^{-\varepsilon_w}F_{2,t+1}^{w}\right]. \tag{A.38}$$

The aggregate wage defined by (19) satisfies the following condition:

$$\theta_w\left(\frac{\bar{\pi}_t}{\pi_t^{w}}\right)^{1-\varepsilon_w} + (1-\theta_w)\omega_w\left(\frac{\left(\pi_{t-1}^{w}\right)^{\gamma_w}(\bar{\pi}_t)^{1-\gamma_w}}{\pi_t^{w}}\right)^{1-\varepsilon_w} + (1-\theta_w)(1-\omega_w)\left(\frac{W_t^{*}}{W_t}\right)^{1-\varepsilon_w} = 1. \tag{A.39}$$

Combining (A.38) with price settings of the optimizing labor unions (A.35), we get

$$\theta_w\left(\frac{\bar{\pi}_t}{\pi_t^{w}}\right)^{1-\varepsilon_w} + (1-\theta_w)\omega_w\left(\frac{\left(\pi_{t-1}^{w}\right)^{\gamma_w}(\bar{\pi}_t)^{1-\gamma_w}}{\pi_t^{w}}\right)^{1-\varepsilon_w} + (1-\theta_w)(1-\omega_w)\left(\frac{w_t^{*}}{w_t}\right)^{1-\varepsilon_w} = 1. \tag{A.40}$$

The marginal utility of consumption (A.30) can be expressed employing (18) as follows:

$$\lambda_t = (C_t-\xi C_{t-1})^{\frac{-1}{\mu}}\exp\left(\frac{\eta(1-\mu)}{\mu(1+\eta)}\int_0^1(L_{ht})^{\frac{\eta+1}{\eta}}dh\right)\eta_t^{c} = (C_t-\xi C_{t-1})^{\frac{-1}{\mu}}\exp\left(\frac{\eta(1-\mu)}{\mu(1+\eta)}\Delta_t^{w}L_t^{\frac{\eta+1}{\eta}}\right)\eta_t^{c}, \tag{A.41}$$

where $\Delta_t^{w} = \int_0^1\left(\frac{W_{ht}}{W_t}\right)^{\frac{-\varepsilon_w(\eta+1)}{\eta}}dh$ is the wage dispersion term. Introducing the following price index

$$\bar{W}_t = \left(\int_0^1(W_{ht})^{\frac{-\varepsilon_w(\eta+1)}{\eta}}dh\right)^{\frac{-\eta}{\varepsilon_w(\eta+1)}},$$

the dynamics of the wage dispersion term can be derived as follows:

$$\left(\frac{\bar{W}_t}{W_t}\right)^{\frac{-\varepsilon_w(\eta+1)}{\eta}} = \theta_w\left(\frac{\bar{\pi}\bar{W}_{t-1}}{W_t}\right)^{\frac{-\varepsilon_w(\eta+1)}{\eta}} + (1-\theta_w)\omega_w\left(\frac{\left(\pi_{t-1}^{w}\right)^{\gamma_w}(\bar{\pi}_t)^{1-\gamma_w}\bar{W}_{t-1}}{W_t}\right)^{\frac{-\varepsilon_w(\eta+1)}{\eta}} + (1-\theta_w)(1-\omega_w)\left(\frac{W_t^{*}}{W_t}\right)^{\frac{-\varepsilon_w(\eta+1)}{\eta}}$$

or

$$\Delta_t^{w} = \theta_w\left(\frac{\bar{\pi}_t}{\pi_t^{w}}\right)^{\frac{-\varepsilon_w(\eta+1)}{\eta}}\Delta_{t-1}^{w} + (1-\theta_w)\omega_w\left(\frac{\left(\pi_{t-1}^{w}\right)^{\gamma_w}(\bar{\pi}_t)^{1-\gamma_w}}{\pi_t^{w}}\right)^{\frac{-\varepsilon_w(\eta+1)}{\eta}}\Delta_{t-1}^{w} + (1-\theta_w)(1-\omega_w)\left(\frac{w_t^{*}}{w_t}\right)^{\frac{-\varepsilon_w(\eta+1)}{\eta}}. \tag{A.42}$$

Appendix B. List of model variables

In Table B.1, we list 49 endogenous model variables. When solving the models, the variables are taken either in levels or in logarithms as stated in the table.

In Table B.2, we list 6 exogenous model variables. Interest rate shocks are in levels, the other shocks are in logarithms.

Table B.1
A list of endogenous model variables

Variable	Symbol	In logarithms
labour input	L_t	yes
capital input	K_t	yes
investment	I_t	yes
commodities used domestically	COM_t^d	yes
import	M_t	yes
capital utilization	u_t	no
capital depreciation	d_t	no
gross production of intermediate good	Z_t^g	yes
net production of intermediate good	Z_t^n	yes
total production	Z_t	yes
consumption	C_t	yes
marginal utility of consumption	λ_t	yes
nominal interest rate	R_t	no
inflation	π_t	yes
consumption Phillips curve term	F_{1t}	yes
consumption Phillips curve term	F_{2t}	yes
price dispersion	Δ_t	yes
real marginal cost	rmc_t	yes
inflation target	$\bar{\pi}_t$	yes
real price of intermediate good	p_t^z	yes
real price of import	p_t^m	yes
foreign price of import	p_t^{mf}	yes
real exchange rate	s_t	yes
imported good inflation	π_t^m	yes
imports Phillips curve term	F_{1t}^m	yes
imports Phillips curve term	F_{2t}^m	yes
wage inflation	π_t^w	yes
wage Phillips curve term	F_{1t}^w	yes
wage Phillips curve term	F_{2t}^w	yes
wage dispersion	Δ_t^w	yes
real wage	w_t	yes
optimal wage	w_t^*	yes
real price of commodities	p_t^{com}	yes
marginal product of capital	MPK_t	yes
interest rate on capital	R_t^k	no
real price of investment	p_t^i	yes
Tobin's Q	q_t	yes
price of non-commodity export	p_t^{xz}	yes
interest premium on foreign bonds	κ_t^f	no
non-commodity export	X_t^{nc}	yes
export of commodities	X_t^{com}	yes
total commodities produced	COM_t	yes
final goods used in commodity production	Z_t^{com}	yes
GDP	Y_t	yes
potential GDP	$\bar{Y}_t$	yes
GDP deflator	p_t^y	yes
holdings of foreign bonds in real terms	b_t^f	no
auxiliary expectation term	ex_t^i	no
auxiliary expectation term	ex_t^{com}	no

Table B.2
A list of exogenous model variables

Variable	Symbol	In logarithms
interest rate shock process	η_t^r	no
productivity	A_t	yes
consumption demand shock process	η_t^c	yes
foreign activity measure	Z_t^f	yes
foreign-currency price of commodities	p_t^{comf}	yes
foreign real interest rate	r_t^f	no

Appendix C. List of model equations

The bToTEM model consists of 49 equations and 49 endogenous variables, as well as 6 exogenous autocorrelative shock processes. Here we summarize all model equations.

- Production of finished goods

- Production technology (1), (5)

$$Z_t^g = \left(\delta_l (A_t L_t)^{\frac{\sigma-1}{\sigma}} + \delta_k (u_t K_t)^{\frac{\sigma-1}{\sigma}} + \delta_{com}\left(COM_t^d\right)^{\frac{\sigma-1}{\sigma}} + \delta_m (M_t)^{\frac{\sigma-1}{\sigma}}\right)^{\frac{\sigma}{\sigma-1}}$$

$$Z_t^n = Z_t^g - \frac{\chi_i}{2}\left(\frac{I_t}{I_{t-1}} - 1\right)^2 I_t$$

- Optimality conditions (A.1), (A.2), (A.3), (A.4), (A.5), (A.6)

$$w_t = p_t^z \left(Z_t^g\right)^{\frac{1}{\sigma}} \delta_l (A_t)^{\frac{\sigma-1}{\sigma}} (L_t)^{\frac{-1}{\sigma}}$$

$$MPK_t = \left(Z_t^g\right)^{\frac{1}{\sigma}} \delta_k (u_t)^{\frac{-1}{\sigma}} (K_t)^{\frac{-1}{\sigma}}$$

$$R_t^k = R_t\left(1 + \kappa_t^k\right)$$

$$q_t = \frac{1}{R_t^k} E_t\left[\pi_{t+1}\left(p_{t+1}^z MPK_{t+1} u_{t+1} + q_{t+1}(1 - d_{t+1})\right)\right]$$

$$p_t^i = q_t - p_t^z \frac{\chi_i}{2}\left(\frac{I_t}{I_{t-1}} - 1\right)\left(\frac{3I_t}{I_{t-1}} - 1\right) + \frac{1}{R_t^k} E_t\left[\pi_{t+1} p_{t+1}^z \chi_i \left(\frac{I_{t+1}}{I_t} - 1\right)\left(\frac{I_{t+1}}{I_t}\right)^2\right]$$

$$p_t^{com} = p_t^z \left(Z_t^g\right)^{\frac{1}{\sigma}} \delta_{com}\left(COM_t^d\right)^{\frac{-1}{\sigma}}$$

$$p_t^m = p_t^z \left(Z_t^g\right)^{\frac{1}{\sigma}} \delta_m (M_t)^{\frac{-1}{\sigma}}$$

$$q_t \bar{d} \rho e^{\rho(u_t - 1)} = p_t^z MPK_t$$

- Law of motion for capital (3), (4)

$$K_t = (1 - d_{t-1}) K_{t-1} + I_{t-1}$$

$$d_t = d_0 + \bar{d} e^{\rho(u_t - 1)}$$

- New-Keynesian Phillips curve for finished goods (A.14), (A.16), (A.17), (A.19)

$$rmc_t = p_t^z (1 - s_m) + s_m$$

$$F_{1t} = \lambda_t Z_t \frac{\varepsilon}{\varepsilon - 1} rmc_t + \beta\theta E_t\left[\left(\frac{\bar{\pi}_{t+1}}{\pi_{t+1}}\right)^{-\varepsilon} F_{1t+1}\right]$$

$$F_{2t} = \lambda_t Z_t + \beta\theta E_t\left[\left(\frac{\bar{\pi}_{t+1}}{\pi_{t+1}}\right)^{1-\varepsilon} F_{2t+1}\right]$$

$$\theta\left(\frac{\bar{\pi}_t}{\pi_t}\right)^{1-\varepsilon} + (1-\theta)\omega\left(\frac{(\pi_{t-1})^{\gamma}(\bar{\pi}_t)^{1-\gamma}}{\pi_t}\right)^{1-\varepsilon} + (1-\theta)(1-\omega)\left(\frac{F_{1t}}{F_{2t}}\right)^{1-\varepsilon} = 1$$

- Price dispersion (11), (A.20)

$$Z_t^n = (1 - s_m)\Delta_t Z_t$$

$$\Delta_t = \theta\left(\frac{\bar{\pi}_t}{\pi_t}\right)^{-\varepsilon} \Delta_{t-1} + (1-\theta)\omega\left(\frac{(\pi_{t-1})^{\gamma}(\bar{\pi}_t)^{1-\gamma}}{\pi_t}\right)^{-\varepsilon} \Delta_{t-1} + (1-\theta)(1-\omega)\left(\frac{F_{1t}}{F_{2t}}\right)^{-\varepsilon}$$

- Commodities
  - Production technology (12)

$$COM_t = (Z_t^{com})^{s_z} (A_t F)^{1-s_z} - \frac{\chi_{com}}{2}\left(\frac{Z_t^{com}}{Z_{t-1}^{com}} - 1\right)^2 Z_t^{com}$$

- Demand (A.22)

$$1 = p_t^{com}\frac{s_z COM_t}{Z_t^{com}} - p_t^{com}\frac{\chi_{com}}{2}\left(\frac{Z_t^{com}}{Z_{t-1}^{com}}-1\right)\left(\frac{3Z_t^{com}}{Z_{t-1}^{com}}-1\right) + \frac{1}{R_t}E_t\left[\pi_{t+1}p_{t+1}^{com}\chi_{com}\left(\frac{Z_{t+1}^{com}}{Z_t^{com}}-1\right)\left(\frac{Z_{t+1}^{com}}{Z_t^{com}}\right)^2\right]$$

- Commodity price (13)

$$p_t^{com} = s_t p_t^{comf}$$

- Households
  - Euler equation (A.29), (A.40)

$$\lambda_t = (C_t - \xi C_{t-1})^{\frac{-1}{\mu}}\exp\left(\frac{\eta(1-\mu)}{\mu(1+\eta)}\Delta_t^w (L_t)^{\frac{\eta+1}{\eta}}\right)\eta_t^c$$

$$\lambda_t = E_t\left[\lambda_{t+1}\frac{\beta R_t}{\pi_{t+1}}\right]$$

  - Wage dispersion (A.41)

$$\Delta_t^w = \theta_w\left(\frac{\bar{\pi}_t}{\pi_t^w}\right)^{\frac{-\varepsilon_w(\eta+1)}{\eta}}\Delta_{t-1}^w + (1-\theta_w)\omega_w\left(\frac{\left(\pi_{t-1}^w\right)^{\gamma_w}(\bar{\pi}_t)^{1-\gamma_w}}{\pi_t^w}\right)^{\frac{-\varepsilon_w(\eta+1)}{\eta}}\Delta_{t-1}^w + (1-\theta_w)(1-\omega_w)\left(\frac{w_t^*}{w_t}\right)^{\frac{-\varepsilon_w(\eta+1)}{\eta}}$$

  - Phillips curve for wage (A.39), (A.35) (A.36), (A.37)

$$\pi_t^w = \frac{w_t}{w_{t-1}}\pi_t$$

$$(w_t^*)^{1+\frac{\varepsilon_w}{\eta}}(w_t)^{\frac{-\varepsilon_w}{\eta}} = \frac{F_{1t}^w}{F_{2t}^w}$$

$$F_{1t}^w = \lambda_t\frac{\varepsilon_w}{\varepsilon_w-1}(C_t-\xi C_{t-1})(L_t)^{\frac{1+\eta}{\eta}} + \beta\theta E_t\left[\left(\frac{\bar{\pi}_{t+1}}{\pi_{t+1}^w}\right)^{\frac{-\varepsilon_w(1+\eta)}{\eta}}F_{1,t+1}^w\right]$$

$$F_{2t}^w = \lambda_t L_t + \beta\theta E_t\left[\frac{\bar{\pi}_{t+1}}{\pi_{t+1}}\left(\frac{\bar{\pi}_{t+1}}{\pi_{t+1}^w}\right)^{-\varepsilon_w}F_{2,t+1}^w\right]$$

$$\theta_w\left(\frac{\bar{\pi}_t}{\pi_t^w}\right)^{1-\varepsilon_w} + (1-\theta_w)\omega_w\left(\frac{\left(\pi_{t-1}^w\right)^{\gamma_w}(\bar{\pi}_t)^{1-\gamma_w}}{\pi_t^w}\right)^{1-\varepsilon_w} + (1-\theta_w)(1-\omega_w)\left(\frac{w_t^*}{w_t}\right)^{1-\varepsilon_w} = 1$$

- Open economy
  - New-Keynesian Phillips curve for imported goods (A.25), (A.26), (A.28)

$$\pi_t^m = \frac{p_t^m}{p_{t-1}^m}\pi_t$$

$$F_{1t}^m = \lambda_t M_t\frac{\varepsilon_m}{\varepsilon_m-1}s_t p_t^{mf} + \beta\theta_m E_t\left[\left(\frac{\bar{\pi}_{t+1}}{\pi_{t+1}^m}\right)^{-\varepsilon_m}F_{1t+1}^m\right]$$

$$F_{2t}^m = \lambda_t M_t + \beta\theta_m E_t\left[\frac{\bar{\pi}_{t+1}}{\pi_{t+1}}\left(\frac{\bar{\pi}_{t+1}}{\pi_{t+1}^m}\right)^{-\varepsilon_m}F_{2t+1}^m\right]$$

$$\theta_m\left(\frac{\bar{\pi}_t}{\pi_t^m}\right)^{1-\varepsilon_m} + (1-\theta_m)\omega_m\left(\frac{\left(\pi_{t-1}^m\right)^{\gamma_m}(\bar{\pi}_t)^{1-\gamma_m}}{\pi_t^m}\right)^{1-\varepsilon_m} + (1-\theta_m)(1-\omega_m)\left(\frac{F_{1t}^m}{p_t^m F_{2t}^m}\right)^{1-\varepsilon_m} = 1$$

  - Foreign demand for noncommodity exports (24)

$$X_t^{nc} = \gamma^f\left(\frac{s_t}{p_t^{nc}}\right)^{\phi}Z_t^f$$

- Interest rate parity (A.31), (35)

$$s_t = E_t\left[\left(s_{t-1}\frac{\pi_t^f}{\pi_t}\right)^{\varkappa}\left(s_{t+1}\frac{r_t^f\left(1+\kappa_t^f\right)}{R_t}\pi_{t+1}\right)^{1-\varkappa}\right]$$

$$\kappa_t^f = \varsigma\left(\bar{b}^f - b_t^f\right)$$

- Balance of payments (27)

$$\frac{b_t^f}{r_t^f\left(1+\kappa_t^f\right)} - b_{t-1}^f\frac{s_t}{s_{t-1}} = \frac{1}{\bar{Y}}\left(p_t^{nc}X_t^{nc} + p_t^{com}X_t^{com} - p_t^m M_t\right)$$

- Monetary policy rule (23)

$$R_t = \left\{R^{elb}, \rho_r R_{t-1} + (1-\rho_r)\left(\bar{R} + \rho_\pi\left(\pi_t - \bar{\pi}_t\right) + \rho_Y\left(\log Y_t - \log\bar{Y}_t\right)\right) + \eta_t^r\right\}$$

- Market clearing conditions (32), (33), (34)

$$Z_t = C_t + \iota_i I_t + \iota_x X_t^{nc} + Z_t^{com} + \upsilon_z Z_t$$

$$Y_t = C_t + I_t + X_t^{nc} + X_t^{com} - M_t + \upsilon_y Y_t$$

$$p_t^y Y_t = C_t + p_t^i I_t + p_t^{nc}X_t^{nc} + p_t^{com}X_t^{com} - p_t^m M_t + \upsilon_y p_t^y Y_t$$

$$COM_t = COM_t^d + X_t^{com}$$

- Exogenous processes
  - Processes for shocks

$$\eta_t^r = \varphi_r\eta_{t-1}^r + \xi_t^r$$

$$\log\left(A_t\right) = \varphi_a\log\left(A_{t-1}\right) + \left(1-\varphi_a\right)\log\left(\bar{A}\right) + \xi_t^a$$

$$\log\left(\eta_t^c\right) = \varphi_c\log\left(\eta_{t-1}^c\right) + \xi_t^c$$

$$\log\left(Z_t^f\right) = \varphi_{zf}\log\left(Z_{t-1}^f\right) + \left(1-\varphi_{zf}\right)\log\left(\bar{Z}^f\right) + \xi_t^{zf}$$

$$\log\left(p_t^{comf}\right) = \varphi_{comf}\log\left(p_{t-1}^{comf}\right) + \left(1-\varphi_{comf}\right)\log\left(\bar{p}^{comf}\right) + \xi_t^{comf}$$

$$\log\left(r_t^f\right) = \varphi_{rf}\log\left(r_{t-1}^f\right) + \left(1-\varphi_{rf}\right)\log\left(\bar{r}\right) + \xi_t^{rf}$$

  - Fixed exogenous prices

$$p_t^i = \iota_i$$

$$p_t^{nc} = \iota_x$$

$$p_t^{mf} = \bar{p}^{mf}$$

  - Targets

$$\bar{\pi}_t = \bar{\pi}$$

$$\log\bar{Y}_t = \varphi_z\log\bar{Y}_{t-1} + (1-\varphi_z)\log\left(\frac{A_t\bar{Y}}{\bar{A}}\right)$$

- Auxiliary expectation terms

$$ex_t^i = E_t\left[\pi_{t+1}p_{t+1}^z\chi_i\left(\frac{I_{t+1}}{I_t}-1\right)\left(\frac{I_{t+1}}{I_t}\right)^2\right]$$

$$ex_t^{com} = E_t\left[\pi_{t+1}p_{t+1}^{com}\chi_{com}\left(\frac{Z_{t+1}^{com}}{Z_t^{com}}-1\right)\left(\frac{Z_{t+1}^{com}}{Z_t^{com}}\right)^2\right]$$

Appendix D. bToTEM parameters

The calibrated values of the parameters for the bToTEM model are summarized in the following two tables.

In Table D.1, we summarize the parameters in the endogenous equations of the model and in Table D.2, we collect the parameters of the exogenous processes for shocks.

Table D.1
Calibrated parameters in endogenous model's equations

Parameter	Symbol	Value	Source
Rates			
– real interest rate	$\bar{r}$	1.0076	ToTEM
– discount factor	β	0.9925	ToTEM
– inflation target	$\bar{\pi}$	1.005	ToTEM
– nominal interest rate	$\bar{R}$	1.0126	ToTEM
– ELB on the nominal interest rate	R^{elb}	1.0076	fixed
Output production			
– CES elasticity of substitution	σ	0.5	ToTEM
– CES labor share parameter	δ_l	0.249	calibrated
– CES capital share parameter	δ_k	0.575	calibrated
– CES commodity share parameter	δ_{com}	0.0015	calibrated
– CES import share parameter	δ_m	0.0287	calibrated
– investment adjustment cost	χ_i	20	calibrated
– fixed depreciation rate	d_0	0.0054	ToTEM
– variable depreciation rate	$\bar{d}$	0.0261	ToTEM
– depreciation semielasticity	ρ	4.0931	calibrated
– real investment price	ι_i	1.2698	ToTEM
– real noncommodity export price	ι_x	1.143	ToTEM
– labor productivity	$\bar{A}$	100	normalization
Price setting parameters for consumption			
– probability of indexation	θ	0.75	ToTEM
– RT indexation to past inflation	γ	0.0576	ToTEM
– RT share	ω	0.4819	ToTEM
– elasticity of substitution of consumption goods	ε	11	ToTEM
– Leontief technology parameter	s_m	0.6	ToTEM
Price setting parameters for imports			
– probability of indexation	θ_m	0.8635	ToTEM
– RT indexation to past inflation	γ_m	0.7358	ToTEM
– RT share	ω_m	0.3	ToTEM
– elasticity of substitution of imports	ε_m	4.4	
Price setting parameters for wages			
– probability of indexation	θ_w	0.5901	ToTEM
– RT indexation to past inflation	γ_w	0.1087	ToTEM
– RT share	ω_w	0.6896	ToTEM
– elasticity of substitution of labor service	ε_w	1.5	ToTEM
Household utility			
– consumption habit	ξ	0.9396	ToTEM
– consumption elasticity of substitution	μ	0.8775	ToTEM
– wage elasticity of labor supply	η	0.0704	ToTEM
Monetary policy			
– interest rate persistence parameter	ρ_r	0.83	ToTEM
– interest rate response to inflation gap	ρ_π	4.12	ToTEM
– interest rate response to output gap	ρ_y	0.4	ToTEM
Other			
– capital premium	κ^k	0.0674	calibrated
– exchange rate persistence parameter	$\varkappa$	0.1585	ToTEM
– foreign commodity price	$\bar{p}^{comf}$	1.6591	ToTEM
– foreign import price	$\bar{p}^{mf}$	1.294	ToTEM
– risk premium response to debt	ς	0.0083	calibrated
– export scale factor	γ^f	18.3113	calibrated
– foreign demand elasticity	ϕ	0.4	calibrated
– elasticity in commodity production	s_z	0.8	calibrated
– land	F	0.1559	calibrated
– share of other components of output	υ_z	0.7651	calibrated
– share of other components of GDP	υ_y	0.311	calibrated
– adjustment cost in commodity production	χ_{com}	16	calibrated
– persistence of potential GDP	φ_z	0.75	calibrated

Table D.2
Calibrated parameters in exogenous model's equations

Parameter	Symbol	Value	Source
Shock persistence			
– persistence of interest rate shock	φ_r	0.25	ToTEM
– persistence of productivity shock	φ_a	0.9	fixed
– persistence of consumption demand shock	φ_c	0	fixed
– persistence of foreign output shock	φ_{zf}	0.9	fixed
– persistence of foreign commodity price shock	φ_{comf}	0.87	calibrated
– persistence of foreign interest rate shock	φ_{rf}	0.88	calibrated
Shock volatility			
– standard deviation of interest rate shock	σ_r	0.0006	calibrated
– standard deviation of productivity shock	σ_a	0.0067	calibrated
– standard deviation of consumption demand shock	σ_c	0.0001	fixed
– standard deviation of foreign output shock	σ_{zf}	0.0085	calibrated
– standard deviation of foreign commodity price shock	σ_{comf}	0.0796	calibrated
– standard deviation of foreign interest rate shock	σ_{rf}	0.0020	calibrated

Appendix E. A comparison of bToTEM to ToTEM

There are three aspects in which bToTEM is simplified relatively to ToTEM.[13] First, the full-scale ToTEM model consists of five distinct production sectors, namely, those for producing consumption goods and services, investment goods, government goods, noncommodity export goods, commodities, and it also has a separate economic model of the rest of the world (ROW). The first four of ToTEM's production sectors have identical production technology and constraints, and only differ in the values of parameters. In the bToTEM model, in place of the four sectors we assume just one production sector, which is identical in structure to the consumption goods and services sector of the ToTEM model, and we introduce linear technologies for transforming the output of this sector into other types of output corresponding to the remaining ToTEM's sectors.

Second, there are three types of households in ToTEM that differ in their saving opportunities. In turn, in bToTEM we assume just one type of household. Like in ToTEM, the bToTEM's households supply differentiated labor services in exchange for sticky wages. Under our assumptions, Phillips curves in bToTEM are identical to those in ToTEM; the difference is that bToTEM has three Phillips curves, while ToTEM has eight Phillips curves.

Finally, in ToTEM, the ROW sector is represented as a separate new Keynesian model with its own production sector, while in bToTEM the ROW sector is modeled by using appropriately calibrated exogenous processes for foreign variables.

The ToTEM model is analyzed by the Bank of Canada with the help of a first-order perturbation method that is implemented by using IRIS software.[14] To compare our bToTEM with ToTEM, we construct a similar first-order perturbation solution to bToTEM.[15] We also include in the comparison the impulse response functions for LENS, which is another model of Canadian economy used the Bank of Canada. LENS is not a general-equilibrium model, i.e., it is not derived from microfoundations like ToTEM and bToTEM. It is a large-scale macroeconometric model composed of a set of equations whose coefficients are estimated from the data and are fixed for some period of time.[16] The inclusion of LENS into the comparison allows us to present the difference between bToTEM and ToTEM relative to the difference between two different central-bank models of the same economy.

In Figs. E.1, E.2, E.3, we plot impulse responses to three domestic shocks in the bToTEM model, namely, an interest rate shock, a consumption demand shock, and a permanent productivity shock, respectively.[17] In the figures, we report the response functions of four key model's variables: the nominal short-term interest rate, the rate of inflation for consumption goods and services, the real effective exchange rate, and the output gap. The responses are shown in percentage deviations from the steady state, except for the interest rate and the inflation rate, which are both shown in deviations from the steady state and expressed in annualized terms. The responses we observe are typical for new Keynesian models. In Fig. E.1, a contractionary monetary policy shock leads to a decline in output through a decline in consumption. The uncovered interest rate parity results in appreciation of the domestic currency. A reduction in the real marginal costs implies a lower price of consumption goods, and hence, lower inflation. In Fig. E.2, a negative shock to the discount factor increases consumption and decreases output. The interest rate that is determined by the Taylor rule increases, and the real exchange rate appreciates. In

[13] The version of ToTEM we work with, known also as TOTEM II, builds on the original ToTEM model in Murchison and Rennison (2006); see also Binette et al. (2004) for an earlier simplified version of the original ToTEM model.

[14] This software is available at http://www.iris-toolbox.com; see Beneš et al. (2015) for its description. See also Laséen and Svensson (2011), Guerrieri and Iacoviello (2015) and Holden (2016) for related methods.

[15] We also used Dynare software and we verified that IRIS and Dynare produce indistinguishable numerical solutions to bToTEM. Dynare software is available at http://www.dynare.org; see Adjemian et al. (2011) for the documentation.

[16] See Gervais, Gosselin (2014) for a technical report about the LENS model.

[17] Both, the ToTEM and LENS models, include more sources of uncertainty than the bToTEM model does, namely, 52 shocks in ToTEM and 98 shocks in LENS.

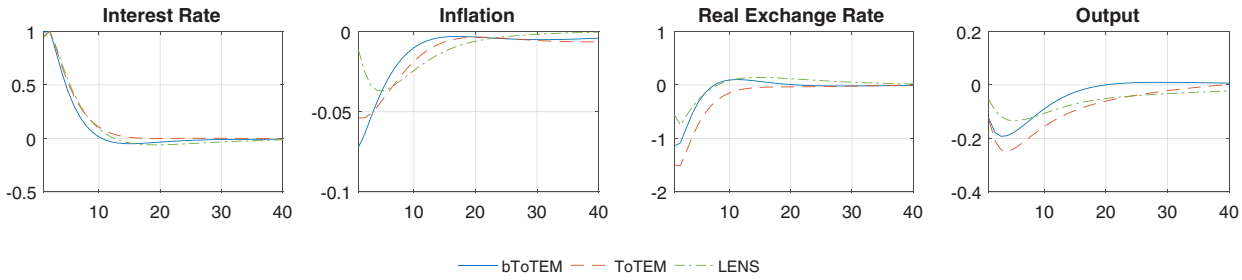

Fig. E.1. Impulse response functions: interest rate shock

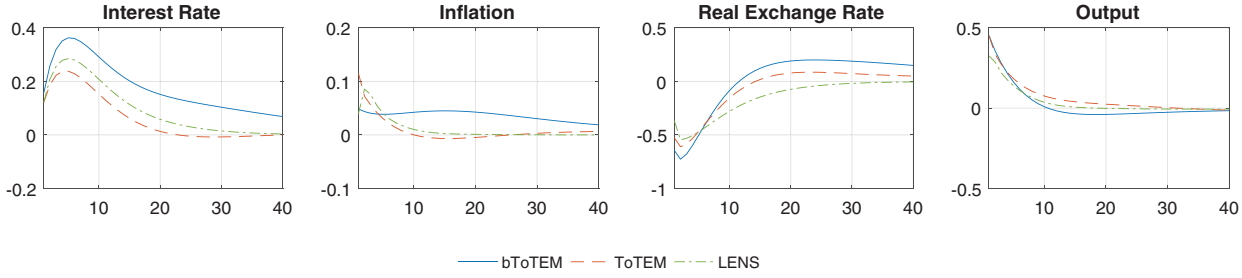

Fig. E.2. Impulse response functions: consumption demand shock

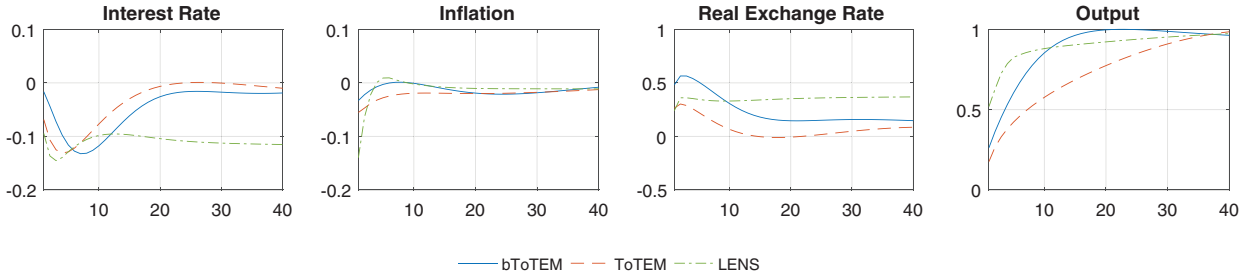

Fig. E.3. Impulse response functions: permanent productivity shock

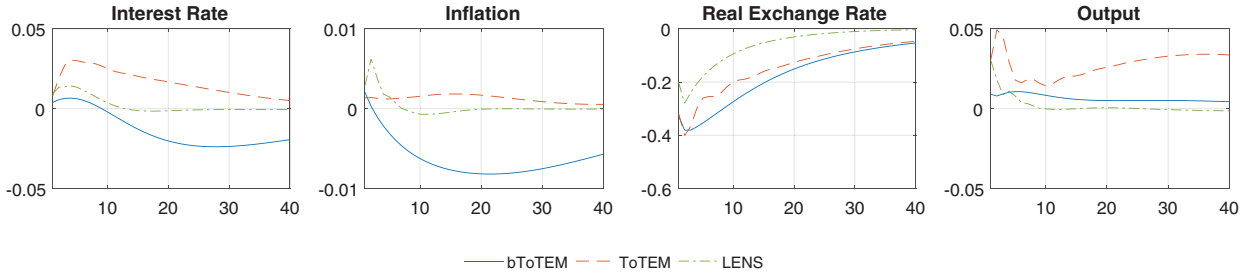

Fig. E.4. Impulse response functions: ROW commodity price shock

Fig. E.3, a permanent increase in productivity gives room for a higher potential output. The actual output gradually increases. Facing a negative output gap, the central bank lowers the interest rate according to the Taylor rule. As actual output reaches the new steady state level, the output gap closes, and the interest rate is back to the neutral rate. A lower interest rate leads to depreciation of the domestic currency because of the interest rate parity. Permanently higher productivity reduces input prices, leading to lower real marginal costs that are reflected in temporary lower inflation.

In Figs. E.4–E.6, we plot impulse responses to three ROW shocks. In Fig. E.4, an increase in the world commodity price leads to an increase in commodity exports as well as to an initial increase in the production costs as commodities are used in the domestic production. An initial increase of inflation is followed in bToTEM by a decline due to an appreciation of domestic currency and a decrease in the price of imports. In Fig. E.5, an increase in the ROW activity measure leads to an increase in noncommodity exports. In turn, it leads to an increase in output and inflation. In Fig. E.6, an increase in the ROW

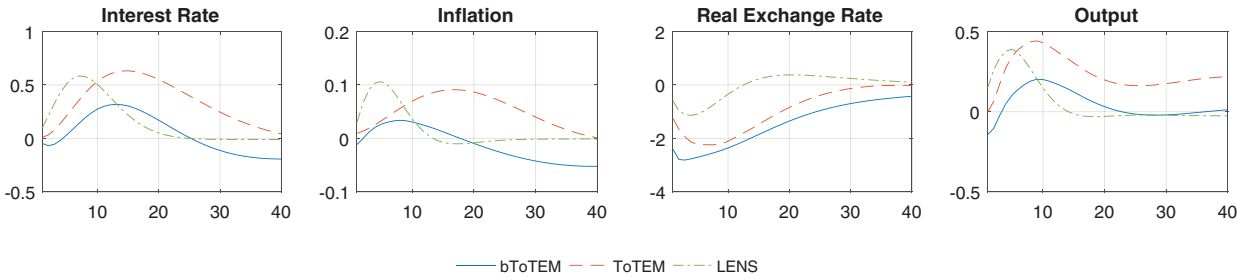

Fig. E.5. Impulse response functions: ROW demand shock

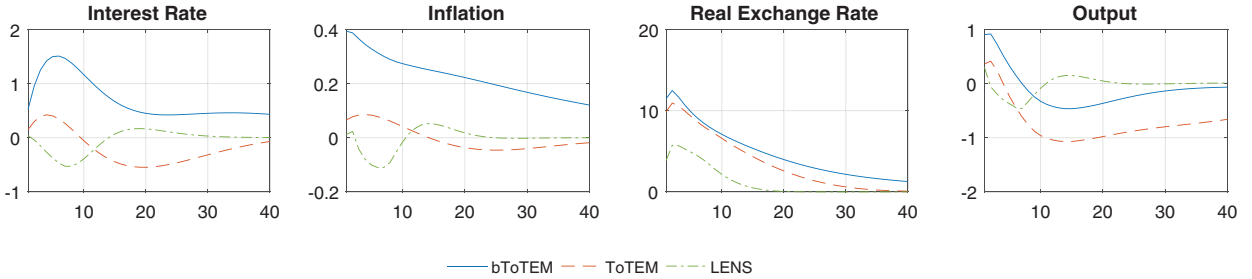

Fig. E.6. Impulse response functions: ROW interest rate shock

interest rate results in a deep depreciation of domestic currency that leads to an increase in exports. An initial increase in output and the interest rate is followed by a decline in consumption that accounts for the following decline in output.

Our main finding is that our bToTEM model replicates the key properties of the full-scale ToTEM model remarkably well. Since ToTEM allows for multiple interest rates, different good prices, fiscal policies, etc., it has a richer structure than bToTEM. However, the variables that are the same in both models are described by essentially the same equations and therefore, have similar dynamics. One noticeable exception is the dynamics of inflation in response to a consumption demand shock; see Fig. 2. In bToTEM, inflation reacts less on the impact, but decreases more slowly than in the other two models. To understand this difference between the two models, let us consider a linearized version of the Phillips curve, which is the same in bToTEM and ToTEM,

$$\hat{\pi}_t = (1-\theta)\gamma\omega\tilde{\phi}^{-1}\hat{\pi}_{t-1} + \beta\theta\tilde{\phi}^{-1}E[\hat{\pi}_{t+1}] + \tilde{\lambda}\hat{rmc}_t + \varepsilon_t^p, \tag{E.1}$$

where rmc_t is the real marginal cost; ε_t^p is a weighted average of the inflation target, the markup, and their expectations, all in deviations from the steady state; θ, γ, ω are the price stickiness parameters defined in Section 2.1; and $\tilde{\phi}$ and $\tilde{\lambda}$ are the parameters defined by equations $\tilde{\phi} = \theta + \omega(1-\theta)(1+\beta\gamma\theta)$ and $\tilde{\lambda} = (1-\omega)(1-\theta)(1-\beta\theta)\tilde{\phi}^{-1}$ (see equations (1.20)–(1.22) in Dorich et al. (2013)). We observe that the difference in inflation dynamics is entirely attributed to the difference in the real marginal cost. In ToTEM, a consumption demand shock triggers a reallocation of inputs into the consumption production sector from the other four sectors. In the presence of adjustment costs, the reallocation raises the real marginal cost. In contrast, in bToTEM, there is one production sector and there are no input adjustment costs. Therefore, the responses and decays of the real marginal cost are less pronounced.

We also observe that the impulse responses of the ToTEM and bToTEM models are generally closer to one another than those produced by the ToTEM and LENS models, the two models of the Bank of Canada. This result is not surprising given that the bToTEM model is a scaled-down version of the ToTEM model, while LENS is a macroeconometric model constructed in a different way. Consequently, our comparison results indicate that bToTEM provides an adequate framework for projection and policy analysis of the Canadian economy and that it can be used as a complement to the two models of the Bank of Canada.

Appendix F. Accuracy evaluation

We assess the accuracy of solution by constructing unit-free residuals in the model's equations on the simulated paths obtained in our experiments. Our choice of points for accuracy evaluation differs from the two conventional choices in the literature, which are a fixed set of points in a multidimensional hypercube (or hypersphere) and a set of points produced by stochastic simulation; see Kollmann et al. (2011). We choose to focus on the path in the experiments because it is precisely

Table F.1
Experiment 1. Residuals in the model's equations on the impulse-response path, *log*10 units

	Maximum residual			Average residual		
	Local 1st order	Local 2nd order	Global DL	Local 1st order	Local 2nd order	Global DL
L_t	-2.16	-2.72	-3.60	-2.89	-3.83	-4.65
K_t	-3.60	-4.04	-4.67	-4.34	-5.30	-5.99
I_t	-3.01	-3.38	-3.52	-4.42	-4.50	-4.84
COM_t^d	-2.17	-2.47	-3.68	-2.92	-3.65	-4.43
M_t	-2.16	-2.94	-3.60	-2.89	-4.05	-4.65
u_t	-2.65	-3.20	-3.89	-3.36	-4.43	-5.16
d_t	-2.10	-2.58	-3.37	-2.78	-3.82	-4.64
Z_t^g	-2.29	-3.03	-3.87	-3.05	-4.13	-4.92
Z_t^n	-2.29	-3.03	-3.87	-3.05	-4.13	-4.92
Z_t	-2.29	-3.04	-3.87	-3.06	-4.12	-4.94
C_t	-3.19	-3.11	-4.01	-3.95	-4.23	-5.11
Y_t	-2.58	-3.17	-3.96	-3.24	-3.96	-4.96
π_t	-4.41	-3.84	-4.14	-5.15	-4.92	-4.57
rmc_t	-2.91	-3.15	-4.04	-3.56	-4.30	-5.04
Δ_t	-4.44	-4.86	-5.38	-5.22	-5.32	-6.22
π_t^m	-2.48	-2.70	-3.99	-3.60	-3.76	-5.00
p_t^m	-2.48	-2.73	-4.13	-3.60	-3.78	-4.58
R_t	-3.82	-3.91	-4.27	-4.51	-4.90	-4.74
p_t^z	-2.45	-2.70	-3.56	-3.10	-3.83	-4.57
w_t	-4.13	-4.45	-4.15	-4.81	-5.38	-4.56
p_t^{com}	-2.40	-1.98	-3.05	-3.39	-3.15	-3.97
MPK_t	-2.24	-2.91	-3.34	-3.02	-4.10	-4.53
R_t^k	-2.88	-3.14	-4.27	-4.14	-4.46	-4.74
κ_t^f	-3.57	-2.44	-4.62	-4.65	-3.51	-5.62
b_t^f	-2.02	-2.27	-3.05	-3.05	-3.09	-3.98
X_t^{nc}	-2.80	-2.38	-3.45	-3.79	-3.55	-4.37
X_t^{com}	-1.76	-2.29	-3.18	-2.51	-3.07	-4.41
COM_t	-2.28	-2.54	-3.40	-3.21	-3.28	-4.77
Z_t^{com}	-2.64	-2.37	-3.40	-3.25	-3.43	-4.67
π_t^w	-3.95	-3.96	-4.61	-4.89	-5.03	-5.81
w_t^*	-3.19	-3.10	-3.71	-3.97	-4.19	-4.48
Δ_t^w	-1.44	-2.22	-3.47	-2.52	-3.46	-4.94
F_{1t}	-3.33	-1.71	-2.83	-3.79	-2.92	-3.89
F_{2t}	-3.41	-1.73	-2.91	-3.84	-2.94	-3.74
F_{1t}^w	-1.92	-1.54	-2.37	-2.68	-2.67	-3.60
F_{2t}^w	-3.11	-1.95	-2.95	-4.00	-3.16	-4.15
F_{1t}^m	-2.40	-1.48	-2.63	-2.61	-2.73	-3.87
F_{2t}^m	-2.46	-1.61	-3.05	-2.96	-2.83	-3.91
q_t	-2.47	-2.69	-2.91	-3.89	-4.14	-4.16
λ_t	-2.32	-1.78	-2.72	-3.59	-3.02	-3.87
s_t	-2.40	-1.98	-3.05	-3.39	-3.15	-3.97
Average	-2.75	-2.76	-3.62	-3.58	-3.86	-4.63
Max	-1.44	-1.48	-2.37	-2.51	-2.67	-3.60

the goal of central bankers to attain a high accuracy of solutions in their policy-relevant experiments (rather than on some hypothetical set of points).

For accuracy evaluation, we use a monomial integration rule with $2N^2+1$ nodes, which is more accurate than monomial rule $2N$ used in the solution procedure, where $N=6$ is the number of the stochastic shocks; see Judd et al. (2011) for a detailed description of these integration formulas.

The approximation errors reported in the table are computed over 40 quarters of the first experiment with a negative foreign demand shock. The unit-free residual in each model's equation is expressed in terms of the variable reported in the table: such a residual reflects the difference between the value of that variable produced by the decision function of the corresponding solution method and the value implied by an accurate evaluation of the corresponding model equation, in which case the residuals are loosely interpreted as approximation errors in the corresponding variables.

The resulting unit free residuals in the model's equations are reported in log 10 units. These accuracy units allow for a simple interpretation, namely, "−2" means the size of approximation errors of $10^{-2}=1$ percent while "−2.5 " means approximation errors between 10^{-2} and 10^{-3}, more precisely, we have $10^{-2.5}\approx 0.3$ percent. The average residuals for the first- and second-degree plain perturbation methods, and the second-degree global method are −3.20, −3.45, and −4.11, respectively, and the maximum residuals are −1.43, −1.44, and −2.09, respectively.

Appendix G. The ELB scenario with mixed foreign and domestic shocks

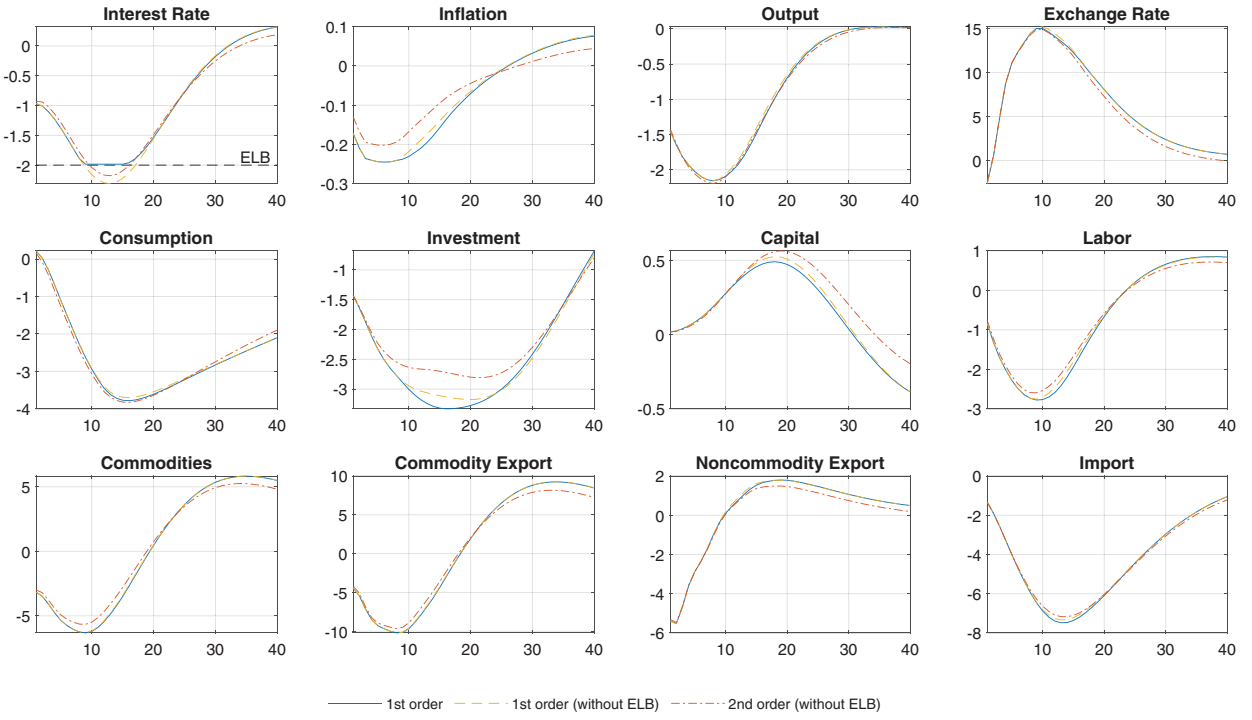

Fig. G.1. Responses of linear and quadratic perturbation solutions in the mixed scenario

Appendix H. Robustness exercises

We conduct three robustness exercises as follows. In the first exercise, we exclude all rule-of-thumb firms and unions by setting ω, ω_w, and ω_m to zero. In the second exercise, we exclude the augmentation from the UIP condition by setting $\varkappa$ to zero. In these two exercises, the dynamic parameter changes have no effect on the deterministic steady state. In the third exercise, we assume that in the second stage of production each firm produces the differentiated final good, Z_{it} from the intermediate good, Z_{it}^n and the manufactured inputs, Z_{it}^{mi} according to the following Cobb-Douglas technology

$$Z_{it} = \left(\frac{Z_{it}^n}{1-s_m}\right)^{1-\alpha_m}\left(\frac{Z_{it}^{mi}}{s_m}\right)^{\alpha_m} \tag{H.1}$$

Then, the real marginal cost is

$$rmc_t = \left(\frac{(1-s_m)p_t^z}{1-\alpha_m}\right)^{1-\alpha_m}\left(\frac{s_m}{\alpha_m}\right)^{\alpha_m}, \tag{H.2}$$

and the aggregated goods in the two stages of production are related as follows:

$$Z_t^n = (1-s_m)^{1-\alpha_m}\left(\frac{s_m(1-\alpha_m)}{\alpha_m p_t^z}\right)^{\alpha_m}\Delta_t Z_t, \tag{H.3}$$

where Δ_t is the price dispersion. We calibrate parameters α_m and s_m to obtain the same deterministic steady state as in the baseline model. The values are $\alpha_m = 0.66$ and $s_m = 0.7168$.

Following the decline of foreign demand in our first experiment, the dynamics of model variables in the three robustness exercises are shown in Fig. H.1.

Our robustness exercises go beyond simple variation in the parameters but involve nontrivial changes in the model's assumptions. Thus, we do not construct fully nonlinear DL solutions for our robustness experiments but restrict our attention to first- and second-order perturbation solutions. Such solutions are easies to construct and experiment with and they are sufficient for deriving useful intuition about the role of the key assumptions in the model's predictions.

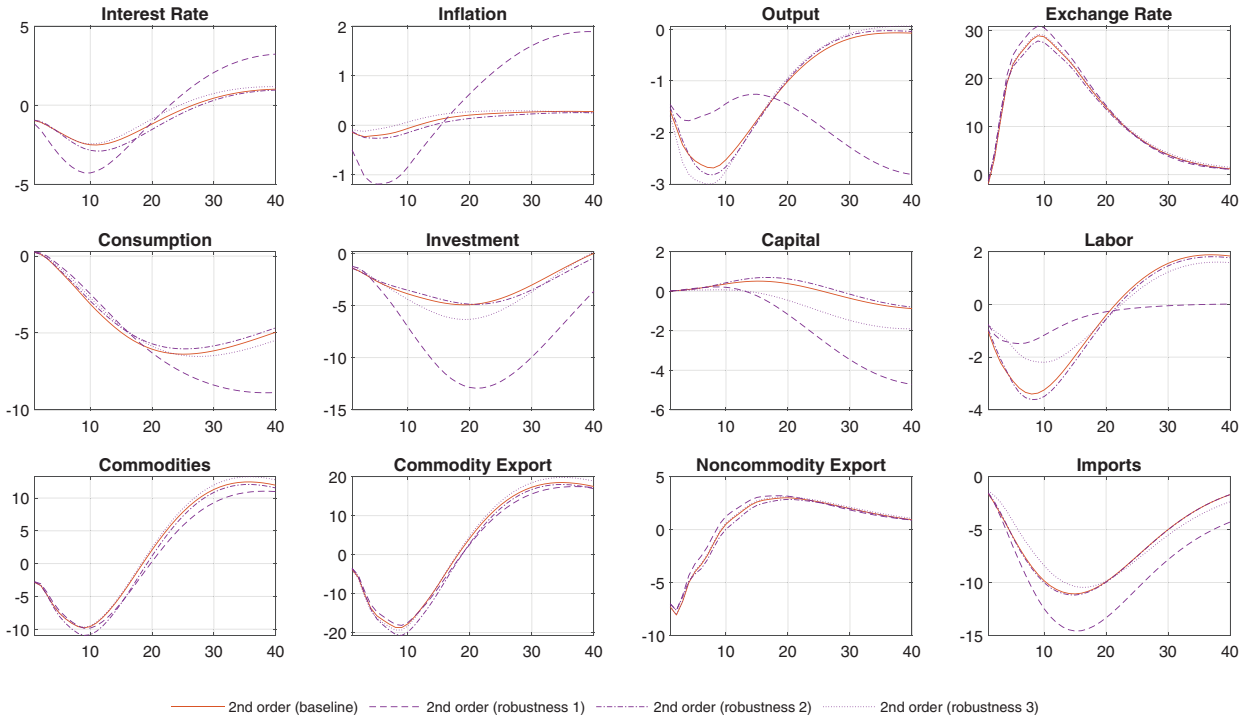

Fig. H.1. Responses of quadratic perturbation solutions to ROW shocks

References

Adjemian, S., Bastani, H., Juillard, M., Mihoubi, F., Perendia, G., Ratto, M., Villemot, S., 2011. Dynare: Reference manual, version 4. Dynare Working Papers, 1, CEPREMAP.

Aruoba, S., Cuba-Borda, P., Schorfheide, F., 2018. Macroeconomic dynamics near ELB: a tale of two countries. Review of Economic Studies 85 (1), 87–118.

Azinović, M., Gaegauf, L., Scheidegger, S., 2019. Deep equilibrium nets. manuscript. SSRN working paper 3393482.

Beneš, J., Johnston, M., Plotnikov, S., 2015. IRIS toolbox release 20151016 (macroeconomic modeling toolbox). Software available at http://www.iris-toolbox.com.

Binette, A., Murchison, S., Perrier, P., Rennison, A., 2004. An introduction to TOTEM. Bank of Canada. Manuscript.

Bodenstein, M., Erceg, C., Guerrieri, L., 2016. The effects of foreign shocks when interest rates are at zero. In: International Finance Discussion Papers 983r. Board of Governors of the Federal Reserve System.

Boivin, J., 2011. The “great” recession in Canada: Perception vs. reality. Speech from March 28 2011.

Boneva, L., Braun, R., Waki, Y., 2016. Some unpleasant properties of log-linearized solutions when the nominal rate is zero. Journal of Monetary Economics 84, 216–232.

Bullard, J., 2013. Seven faces of ’the peril’. Federal Reserve Bank of St. Louis Review. pp. 95

Christiano, L., Eichenbaum, M., Johannsen, B., 2016. Does the new Keynesian model have a uniqueness problem? manuscript.

Christiano, L., Eichenbaum, M., Trabandt, M., 2015. Understanding the great recession. American Economic Journal: Macroeconomics 7 (1), 110–167.

Chung, H., Laforte, J., Reifschneider, D., Williams, J.C., 2012. Have we underestimated the likelihood and severity of zero lower bound events? Journal of Money, Credit and Banking 44, 47–82. (Supplement 1)

Cook, D., Devereux, M., 2016. Exchange rate flexibility under the zero lower bound. Journal of International Economics 101, 52–69.

Corsetti, G., Kuester, K., Müller, G., 2016. The case for flexible exchange rates in a great recession. Manuscript.

Debortoli, D., Galí, J., Gambetti, L., 2019. On the empirical (ir)relevance of the zero lower bound constraint. NBER Macroeconomics Annual 34, 141–170.

Den Haan, W., Marcet, A., 1990. Solving the stochastic growth model by parameterized expectations. Journal of Business and Economic Statistics, 8, 31–34.

Dorich, J., Johnston, M., Mendes, R., Murchison, S., Zhang, Y., 2013. ToTEM II: An updated version of the Bank of Canada’s Quarterly Projection Model. Bank of Canada Technical report no. 100.

Dorich, J., Labelle, N., Lepetyuk, V., Mendes, R., 2018. Could a higher inflation target enhance macroeconomic stability? Canadian Journal of Economics 51 (3), 1029–1055.

Duarte, V., 2018. Machine learning for continuous-time economics. Manuscript.

Duffy, J., McNelis, P., 2001. Approximating and simulating the real business cycle model: parameterized expectations, neural networks, and the genetic algorithm. Journal of Economic Dynamics and Control 25 (9), 1273–1303.

Eggertsson, G. B., Singh, S. R., 2016. Log-linear approximation versus an exact solution at ELB in the new keynesian model. NBER Working Paper 22784.

Fernández-Villaverde, J., Hurtado, S., Nuño, G., 2019. Financial frictions and the wealth distribution. Manuscript.

Fernández-Villaverde, J., Gordon, G., Guerrón-Quintana, P., Rubio-Ramírez, J., 2015. Nonlinear adventures at the zero lower bound. Journal of Economic Dynamics and Control 57, 182–204.

Fernandez, A., Schmitt-Grohé, S., Uribe, M., 2017. World shocks, world prices, and business cycles: an empirical investigation. Journal of International Economics 108, S2–S14. Supplement 1

Galí, J., Gertler, M., 1999. Inflation dynamics: A structural econometric analysis. Journal of Monetary Economics 44 (2), 195–222.

Gervais, O., Gosselin, M., 2014. Analyzing and forecasting the Canadian economy through the LENS model. Bank of Canada Technical report no. 102.

Goodfellow, I., Bengio, Y., Courville, A., 2016. Deep Learning. Massachusetts Institute Technology Press.

Guerrieri, L., Iacoviello, M., 2015. OccBin: A toolkit for solving dynamic models with occasionally binding constraints easily. Journal of Monetary Economics 70, 22–38.

Gust, C., Lopez-Salido, D., Smith, M., 2012. The empirical implications of the interest-rate lower bound. Federal Reserve Board, Finance and Economics Discussion Series. No. 2012–83
Hills, T., Nakata, T., Schmidt, S., 2016. The risky steady state and the interest rate lower bound. Finance and Economics Discussion Series 2016–009. Board of Governors of the Federal Reserve System.
Holden, T., 2016. Computation of solutions to dynamic models with occasionally binding constraints. University of Surrey. Manuscript
Judd, K., Maliar, L., Maliar, S., 2011. Numerically stable and accurate stochastic simulation approaches for solving dynamic models. Quantitative Economics 2 (2), 173–210.
Judd, K., Maliar, L., Maliar, S., 2017. Lower bounds on approximation errors to numerical solutions of dynamic economic models. Econometrica 85 (3), 991–1012.
Kollmann, R., Maliar, S., Malin, B., Pichler, P., 2011. Comparison of solutions to the multi–country real business cycle model. Journal of Economic Dynamics and Control 35, 186–202.
Krusell, P., Smith, A., 1998. Income and wealth heterogeneity in the macroeconomy. Journal of Political Economy 106, 868–896.
Kryvtsov, O., Mendes, R., 2015. The optimal level of the inflation target: a selective review of the literature and outstanding issues. Bank of Canada Staff. Discussion Paper 2015-8
Laséen, S., Svensson, L., 2011. Anticipated alternative policy rate paths in policy simulations. International Journal of Central Banking 7 (3), 1–35.
Leahy, J., 2013. Like a good neighbor: the importance of non–linearities and expectations in the recent crisis. International Journal of Central Banking 9 (2), 287–293.
Lepetyuk, V., Maliar, L., Maliar, S., 2017. Should central banks worry about nonlinearities of their large-scale macroeconomic models? Bank of Canada Staff Working Paper, 2017–21.
Maliar, L., Maliar, S., Winant, P., 2019. Will artificial intelligence replace computational economists any time soon? CEPR discussion paper DP14024.
Maliar, L., Maliar, S., 2014. Numerical methods for large scale dynamic economic models. In: Schmedders, K., Judd, K. (Eds.), Handbook of Computational Economics, Vol. 3. Elsevier Science, Amsterdam.
Maliar, L., Maliar, S., 2015. Merging simulation and projection approaches to solve high-dimensional problems with an application to a new keynesian model. Quantitative Economics 6 (1), 1–47.
Maliar, L., Maliar, S., Judd, K.L., 2011. Solving the multi-country real business cycle model using ergodic set methods. Journal of Economic Dynamic and Control 35 (2), 207–228.
Maliar, L., Maliar, S., Winant, P., 2018. Deep learning for solving dynamic economic models. Video recording of the CEF-2018 conference presentation. https://www.youtube.com/watch?v=u7_CdytTEe8.
Murchison, S., Rennison, A., 2006. ToTEM: The Bank of Canada's new quarterly projection model. Bank of Canada Technical report no. 97.
Schmitt-Grohé, S., Uribe, M., 2003. Closing small open economy models. Journal of International Economics 61, 163–185.
Schmitt-Grohé, S., Uribe, M., 2004. Solving dynamic general equilibrium models using a second-order approximation to the policy function. Journal of Economic Dynamics and Control 28 (4), 755–775.
Smets, F., Wouters, R., 2007. Shocks and frictions in US business cycles: A bayesian DSGE approach. American Economic Review 97 (3), 586–606.
Villa, A., Valaitis, V., 2019. Machine learning projection methods for macro-finance models. Manuscript.